JOURNAL OF GEOPHYSICAL RESEARCH, VOL. 114, B12304, doi:10.1029/2008JB006217, 2009

Shear wave velocity structure of the lower crust in southern Africa: Evidence for compositional heterogeneity within Archaean and Proterozoic terrains

Eldridge M. Kgaswane,[1,2] Andrew A. Nyblade,[3] Jordi Julià,[3] Paul H. G. M. Dirks,[2,4] Raymond J. Durrheim,[2,5] and Michael E. Pasyanos[6]

Received 18 November 2008; revised 29 June 2009; accepted 19 August 2009; published 15 December 2009.

[1] The nature of the lower crust across the southern African shield has been investigated by jointly inverting receiver functions and Rayleigh wave group velocities for 89 broadband seismic stations located in Botswana, South Africa and Zimbabwe. For large parts of both Archaean and Proterozoic terrains, the velocity models obtained from the inversions show shear wave velocities $\geq$4.0 km/s below $\sim$20–30 km depth, indicating a predominantly mafic lower crust. However, for much of the Kimberley terrain and adjacent parts of the Kheis Province and Witwatersrand terrain in South Africa, as well as for the western part of the Tokwe terrain in Zimbabwe, shear wave velocities of $\leq$3.9 km/s are found below $\sim$20–30 km depth, indicating an intermediate-to-felsic lower crust. The areas of intermediate-to-felsic lower crust in South Africa coincide with regions where Ventersdorp rocks have been preserved, suggesting that the more evolved composition of the lower crust may have resulted from crustal reworking and extension during the Ventersdorp tectonomagmatic event at c. 2.7 Ga.

Citation: Kgaswane, E. M., A. A. Nyblade, J. Julià, P. H. G. M. Dirks, R. J. Durrheim, and M. E. Pasyanos (2009), Shear wave velocity structure of the lower crust in southern Africa: Evidence for compositional heterogeneity within Archaean and Proterozoic terrains, *J. Geophys. Res.*, *114*, B12304, doi:10.1029/2008JB006217.

1. Introduction

[2] Motivated by previous studies suggesting that there may be significant variability in the composition of the lower crust across the southern African shield, here we investigate the nature of both Archaean and Proterozoic lower crust in southern Africa using 1-D shear wave velocity models obtained by jointly inverting receiver functions and Rayleigh wave group velocities. Characterizing the variability in lower crustal composition across southern Africa is important not only for improving our understanding of crustal growth and tectonics in Africa, but also globally. As many studies have shown, the composition of the lower crust remains one of the largest unknowns in the overall structure of the crust, leading to considerable uncertainty in the role of the lower crust in continental dynamics [e.g., *Christensen and Mooney*, 1995; *Rudnick and Fountain*, 1995; *Rudnick and Gao*, 2003].

[3] Much of the evidence for variability in lower crustal composition across southern Africa comes from interpreting seismic data. *Niu and James* [2002], for example, using receiver function analysis, found that the lower crust around the Kimberley region in the western part of the Kaapvaal Craton has an intermediate-to-felsic composition. From this result, they suggested that the lower crust beneath the Kaapvaal Craton could be dominated by intermediate-to-felsic lithologies. Receiver function analyses by *Nguuri* [2004] and *Nair et al.* [2006], however, yielded crustal Vp/Vs ratios as high as 1.78 for parts of the Kaapvaal Craton and surrounding Proterozoic mobile belts, suggesting that in some areas the lower crust may contain a significant proportion of mafic rock. Crustal velocity models developed using seismic reflection and refraction data also suggest significant variability in lower crustal composition [e.g., *Green and Durrheim*, 1990; *Durrheim and Green*, 1992; *de Wit and Tinker*, 2004].

[4] The 1-D shear wave velocity models obtained from jointly inverting receiver functions and Rayleigh wave group velocities span the greater part of the exposed Precambrian shield of southern Africa (Figures 1 and 2) and indicate considerable differences in lower crustal composition within and between a number of terrains. In this paper, following a brief review of the geological framework of southern Africa, we describe the data sets and technique used for the joint inversions, discuss similarities and differences in lower

[1]Council for Geoscience, Pretoria, South Africa.
[2]School of Geosciences, University of the Witwatersrand, Johannesburg, South Africa.
[3]Department of Geosciences, Pennsylvania State University, University Park, Pennsylvania, USA.
[4]School of Earth and Environmental Sciences, James Cook University, Townsville, Queensland, Australia.
[5]Council for Scientific and Industrial Research, Johannesburg, South Africa.
[6]Lawrence Livermore National Laboratory, Livermore, California, USA.

0148-0227/09/2008JB006217$09.00

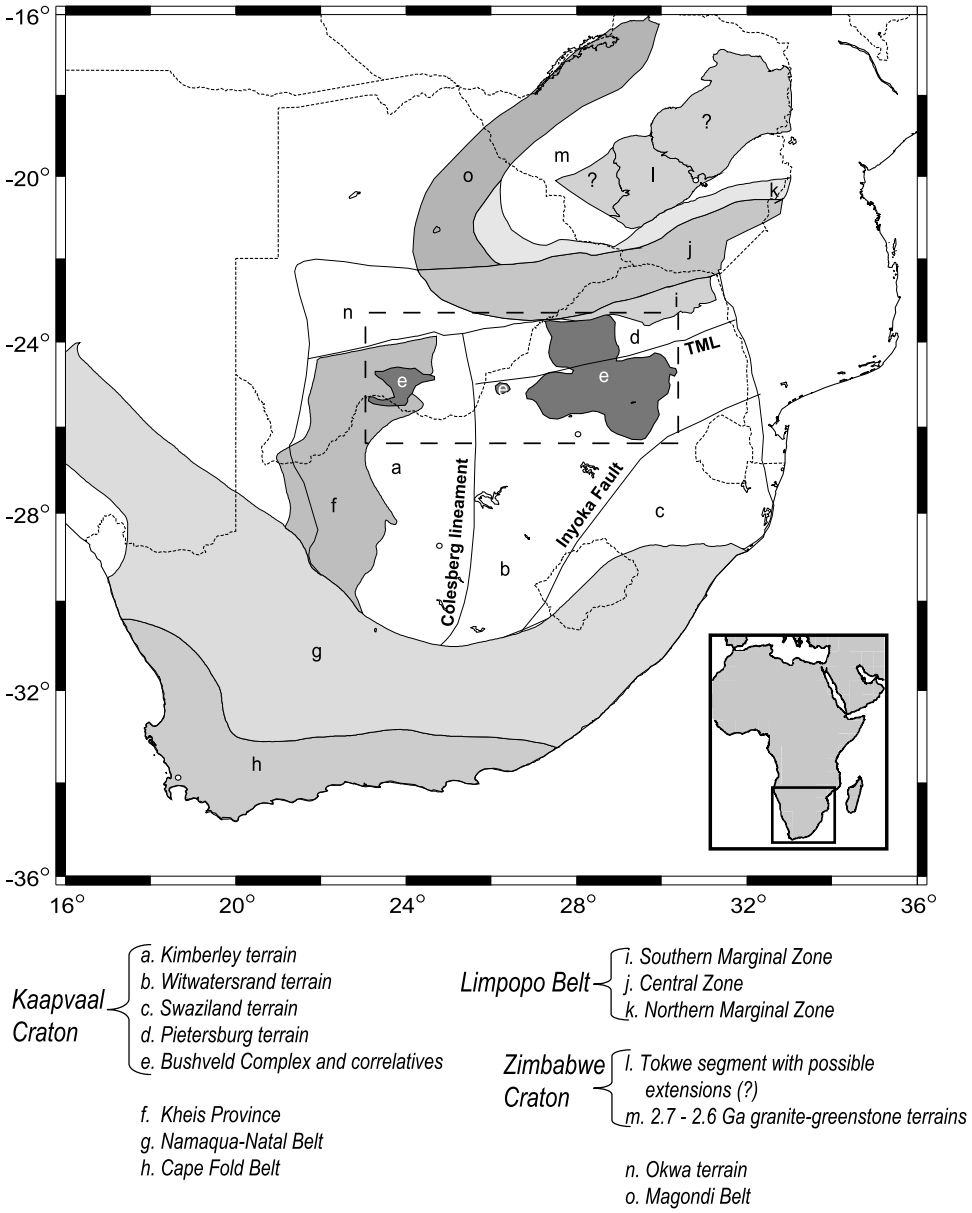

Figure 1. Tectonic map of southern Africa showing major Precambrian terrains. Terrain names and boundaries are taken from *Eglington and Armstrong* [2004] and *Jelsma and Dirks* [2002]. Political boundaries are shown with thin dashed lines. The box shown with bold dashed lines encloses the region affected by the Bushveld Complex. TML, Thabazimbi Murchison Lineament.

crustal composition indicated by the velocity models, and examine possible causes for the lower crustal heterogeneity that we observe vis-à-vis major Precambrian tectonothermal events that affected the region.

2. Tectonic and Geological Framework of Southern Africa

2.1. Overview of Precambrian Structure

[5] The Kalahari Craton, which forms the nucleus of the southern African shield, is comprised of the Archaean Kaapvaal Craton welded to the Archaean Zimbabwe Craton by the Archaean and Palaeoproterozoic Limpopo Belt [*de Wit et al.*, 1992] (Figure 1). The Kalahari Craton is bounded by the Palaeoproterozoic Okwa-Magondi Belt to the northwest, the Mesoproterozoic Namaqua-Natal Belt, including Kheis Province, to the south and southwest, and the Palaeozoic Cape Fold Belt even further to the south (Figure 1). A brief description of these tectonic terrains follows.

2.2. Kaapvaal Craton

[6] The Kaapvaal Craton is an Archaean granite-greenstone terrain that formed between 3.7 and 2.7 Ga [*de Wit et al.*, 1992; *Eglington and Armstrong*, 2004]. Based on the age distribution of supracrustal and intrusive rocks, and the presence of major structural boundaries, the craton has been subdivided into four tectonostratigraphic terrains; the

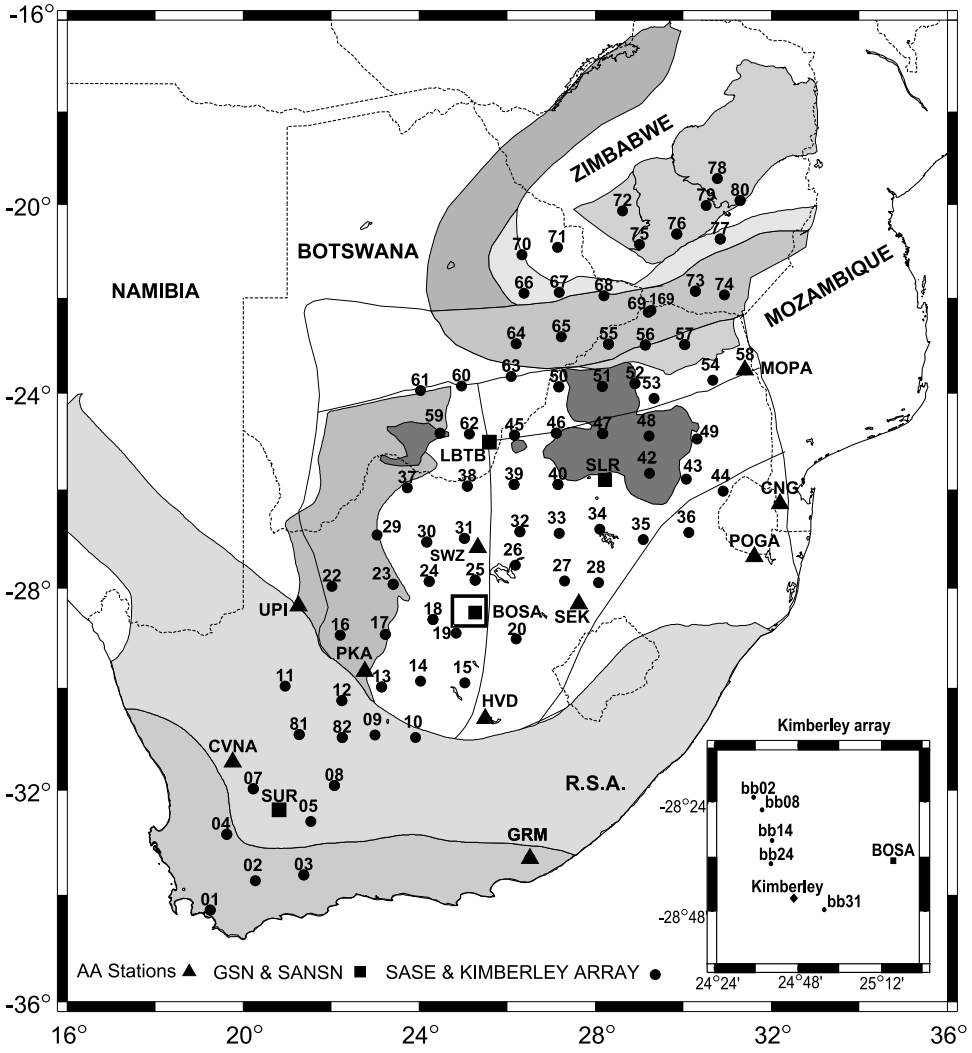

Figure 2. Map showing distribution of broadband seismic stations used in this study in relation to the terrain boundaries shown in Figure 1. The open square in the central part of the Kimberley terrain shows the location of the Kimberley array. The area within the box is enlarged in map in the bottom right corner. AA, AfricaArray network; GSN, Global Seismic Network; SANSN, South Africa National Seismic Network; SASE, Southern African Seismic Experiment.

Kimberley (3.0–2.8 Ga), the Pietersburg (3.0–2.8 Ga), the Witwatersrand and Swaziland terrains (3.6–3.1 Ga) separated by the Thabazimbi-Murchison and Colesburg lineaments and the Inyoka Fault (Figure 1) [*de Wit et al.*, 1992; *Eglington and Armstrong*, 2004]. The Swaziland terrain is the oldest (>3.2 Ga) and the Witwatersrand terrain was accreted to it at ~3.2 Ga. The Pietersburg and Kimberely terrains were joined to the Witwatersrand-Swaziland terrain between 3.0 and 2.8 Ga. Other tectonothermal events that affected the craton are represented by a series of rift-related, intracratonic basins, including the Dominion (3.1 Ga), Witwatersrand (3.0–2.8 Ga), Ventersdorp (2.7 Ga), Transvaal (2.6–2.2 Ga) and Waterberg (2.0–1.8 Ga) basins, and the emplacement of the Bushveld Complex (2.05 Ga) [*Eglington and Armstrong*, 2004; *Johnson et al.*, 2006].

2.3. Zimbabwe Craton

[7] The Zimbabwe Craton consists of granite-greenstone terrains that formed between 3.6 and 2.5 Ga in three stages of crustal formation [e.g., *Dirks and Jelsma*, 2002]. The Tokwe Gneiss terrain in the center of the craton, which formed at 3.6–3.3 Ga, contains mafic fragments that represent the remnants of highly deformed and metamorphosed greenstone belts. A sequence of clastic sediments and greenstones accreted against the western part of the Tokwe Gneiss terrain between 3.2 and 2.8 Ga. The principal period of greenstone formation and accretion occurred between 2.7 and 2.6 Ga, with stabilization of the craton around 2.6 Ga. The Great Dyke was emplaced around 2.58 Ga, marking the last major tectonothermal event to affect the craton [*Jelsma and Dirks*, 2002].

2.4. Limpopo Belt

[8] The Limpopo Belt is a roughly east-west trending zone of high-grade metamorphic rocks that separates the Kaapvaal and Zimbabwe Cratons [e.g., *McCourt and Armstrong*, 1998; *Kramers et al.*, 2006]. The belt has been subdivided into three domains, the Northern Marginal Zone (NMZ), the

Central Zone (CZ) and the Southern Marginal Zone (SMZ), separated by major shear zones [*Kramers et al.*, 2006]. The NMZ and SMZ contain remnants of Archaean granite-greenstone terrains that were modified by a major orogenic event at 2.6–2.5 Ga during which the rocks attained amphibolite to granulite facies metamorphism [e.g., *Berger et al.*, 1995; *Kreissig et al.*, 2000; *Kramers et al.*, 2006]. The CZ (>3.0 and 2.6 and 2.0 Ga) is dominated by granulite facies gneiss with minor metasedimentary and ultramafic intercalations [e.g., *Barton et al.*, 1979; *Kramers et al.*, 2006] affected by orogenic activity at 2.6–2.5 Ga and then again, importantly, at 2.0 Ga, during which the CZ, the NMZ and the SMZ attained their current configuration.

2.5. Bushveld Complex

[9] The Bushveld Complex (BC) (2.05 Ga) is the largest known layered mafic intrusion, extending >350 km in both north-south and east-west directions across the northern Kaapvaal Craton, and reaching a vertical thickness of about 8 km [e.g., *Webb et al.*, 2004] (Figure 1). The intrusion is divided into the Rustenburg Mafic Layered Suite, the Lebowa Granite Suite, the Rashoop Granophyre Suite, and the Rooiberg Group, which consists of rhyolites and basaltic andesites [*South African Committee for Stratigraphy*, 1980; *Hatton and Schweitzer*, 1995; *Cawthorn et al.*, 2006].

2.6. Mesoproterozoic to Palaeozoic Mobile Belts

[10] The Magondi Belt (~2.0–1.8 Ga) to the west and northwest of the Zimbabwe Craton is dominated by passive margin, shelf sediments of the Magondi supergroup thrust eastward onto the craton during the Magondi Orogeny [*McCourt et al.*, 2001]. Magondi Belt rocks have been correlated with deformed mafic and felsic magmatic rocks of the 2.05 Ga Okwa terrain in central Botswana (Figure 1) [*Stowe*, 1989], suggesting the presence of a continuous northeast trending orogenic belt to the west of the Zimbabwe Craton, possibly merging with the CZ of the Limpopo Belt.

[11] The Namaqua-Natal Belt (NNB) to the south and west of the Kaapvaal Craton is comprised of igneous and supracrustal rocks that accreted against the craton during the Namaqua Orogeny (1.2–1.0 Ga). The NNB is exposed to the west (the Namaqua Sector) and southeast (the Natal Sector) of the craton [*Cornell et al.*, 2006], but the central part of the belt is covered by younger sediments of the Karoo Supergroup. The Namaqua Sector is composed of five distinct terrains with ages between 2.0 to 1.3 Ga. These terrains are separated from the Kaapvaal Craton by a passive margin sequence of siliciclastic rocks of the Olifantshoek Supergroup (2.0–1.7 Ga), referred to as the Kheis Province [*Cornell et al.*, 2006]. Accretion of the Namaqua Sector to the craton at 1.0–1.2 Ga coincided with eastward thrusting of Olifantshoek sediments onto the craton [*Moen*, 1999; *Eglington and Armstrong*, 2004], resulting in a thin-skinned fold-and-thrust belt, called the Kheis Belt. The Kheis Belt has been correlated with the Okwa terrain and Magondi Belt to the north [e.g., *Stowe*, 1986], but this correlation is in doubt in light of recent dating summarized by *Cornell et al.* [2006].

[12] The Cape Fold Belt (CFB) is comprised of the siliciclastic passive margin Cape Supergroup (500–330 Ma) [*Thamm and Johnson*, 2006], deformed in a northeast verging fold-and-thrust belt during the Cape Orogeny (~278–245 Ma). The belt is thought to have formed as a result of a subduction zone along the southern margin of the Gondwana supercontinent and also resulted in the formation of the Karoo foreland basin [e.g., *Ransome and de Wit*, 1992; *Newton et al.*, 2006].

3. Seismic Structure of Southern African Crust

[13] Early studies of the crust in the Kaapvaal Craton mainly used seismic recordings of mine tremors associated with gold mining activity in the Witwatersrand basin [e.g., *Gane et al.*, 1949; *Willmore et al.*, 1952; *Gane et al.*, 1956; *Hales and Sacks*, 1959]. *Hales and Sacks* [1959] describe a two-layered crust in the eastern Kaapvaal Craton with a Moho depth of 37 km and a ~24 km thick upper crustal layer with P and S wave velocities of 6.0 and 3.6 km/s, respectively. They also found a lower crustal layer ~13 km thick with P and S wave velocities of 7.0 and 4.0 km/s, respectively. In an early surface wave study, *Bloch et al.* [1969] inverted Rayleigh and Love wave group and phase velocities from regional earthquakes and obtained a Poisson's ratio of 0.28 for the lower crust in the northern Kaapvaal Craton and a crustal thickness in the range of 40–45 km. The first seismic refraction studies in and around the Witwatersrand basin yielded a crustal thickness of 35 km and lower crustal P wave velocities in the range of 6.4 to 6.7 km/s [*Durrheim and Green*, 1992]. A similar study by *Green and Durrheim* [1990] of the NNB obtained a Moho depth of 42 km and lower crustal P wave velocities in the range 6.6 to 6.9 km/s.

[14] More recently, crustal structure in southern Africa has been investigated using data from the Southern African Seismic Experiment (SASE) [*Carlson et al.*, 1996]. A compilation of results from *Harvey et al.* [2001], *Nguuri et al.* [2001], *Stankiewicz et al.* [2002], *Niu and James* [2002], *James et al.* [2003], *Kwadiba et al.* [2003], *Wright et al.* [2003], *Webb et al.* [2004], and *Nair et al.* [2006] show crustal thicknesses of 35–45 km and 34–37 km, respectively, for the Kaapvaal and Zimbabwe cratons. The studies reported Moho depths for the Kheis Province, BC, Limpopo Belt, Okwa/Magondi Belt, NNB and CFB of 40 km, 40–53 km, 37–55 km, 40–45 km, 40–50 km and 26–45 km, respectively.

[15] *Nguuri* [2004] and *Nair et al.* [2006] reported variable Vp/Vs ratios for a number of crustal terrains across southern Africa (Table 1) and interpreted Vp/Vs ratios > 1.76 to be indicative of mafic and ultramafic lithologies in the crust. The differences in the Vp/Vs ratio for some terrains, as well as the number of stations used to compute the average ratios, reflect different selections of geographic regions and data in the two studies. One of the most detailed investigations of crustal structure in the Kaapvaal Craton has been undertaken by *Niu and James* [2002] for a small area in the Kimberley terrain using data from the Kimberley seismic array. *Niu and James* [2002] obtained for the lowermost crust P and S velocities of 6.75 and 3.90 km/s, respectively, and a Poisson's ratio of 0.25, indicating an intermediate-to-felsic composition for the lowermost crust. They also found a sharp (i.e., less than 0.5 km wide) and flat (i.e., topographic relief less than 1 km) Moho. Petrologic studies of the Kimberley area by *Schmitz and Bowring* [2003a, 2003b] show that mafic granulites are absent from

Table 1. Summary of Average Vp/Vs Ratios of the Geological Terrains in Southern Africa

	Kaapvaal Craton		Zimbabwe Craton		Bushveld Complex		Namaqua-Natal Belt		Limpopo Belt		Kheis terrain	
	Vp/Vs	Stations[a]	Vp/Vs	Stations[a]	Vp/Vs	Stations[a]	Vp/Vs	Stations[a]	Vp/Vs	Stations[a]	Vp/Vs	Stations[a]
Nguuri [2004]	1.72 ± 0.05	35	-	-	1.79 ± 0.06	14	1.78 ± 0.05	10	1.84 ± 0.06	12	1.74 ± 0.06	4
Nair et al. [2006]	1.74 ± 0.01	25	1.73 ± 0.01	5	1.78 ± 0.02	5	1.72 ± 0.01	5	1.74 ± 0.01	4	1.73 ± 0.01	4

[a]Number of stations.

lower crustal xenolith suites, consistent with the findings of *Niu and James* [2002].

4. Sources of Data

[16] Broadband seismic data from a total of 101 seismic stations were initially used in this study to compute receiver functions, however, as discussed in section 6, results from only 89 stations are presented and used for interpretation. The stations belong to the SASE network (82 stations), the AfricaArray network (10 stations), the South Africa National Seismic Network (1 station) and the Global Seismic Network (3 stations) (Figure 2). The SASE network was deployed over 2 years (1997–1999) (Figure 2), and data from five stations in the Kimberley array (1999), which was operated as a high resolution extension to the SASE network [*Niu and James*, 2002], were also used. The AfricaArray network began operation in 2006 and consists of permanent seismic stations spread across eastern and southern Africa. More than 1 year of data from the AfricaArray stations in southern Africa were used for this study (Figure 2). A total of 89 teleseismic earthquakes with epicentral distances between 30° and 99° recorded by the stations were selected for computing receiver functions (Figure 3). The earthquakes have moment magnitudes ranging from 5.8 to 9.0.

[17] Rayleigh wave group velocities used in this study for periods of 10 to 90 s were taken from a revised version of the model presented by *Pasyanos and Nyblade* [2007]. In the revised *Pasyanos and Nyblade* [2007] model, group velocity measurements from 39 broadband seismic stations spread across southern Africa were combined with the measurements used for constructing the original *Pasyanos and Nyblade* [2007] model (Figure 4). The group velocity

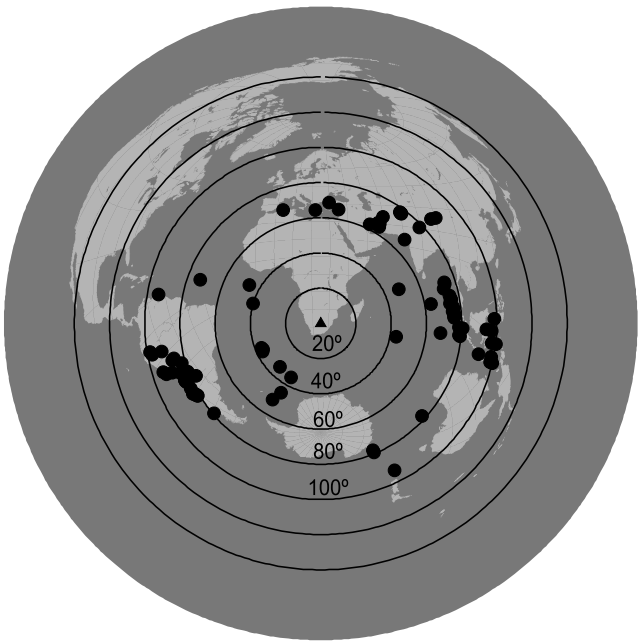

Figure 3. Distribution of teleseismic earthquakes used for this study (small solid circles). The triangle shows the center of the SASE network. Large circles show distance in 20° increments from the center of the network.

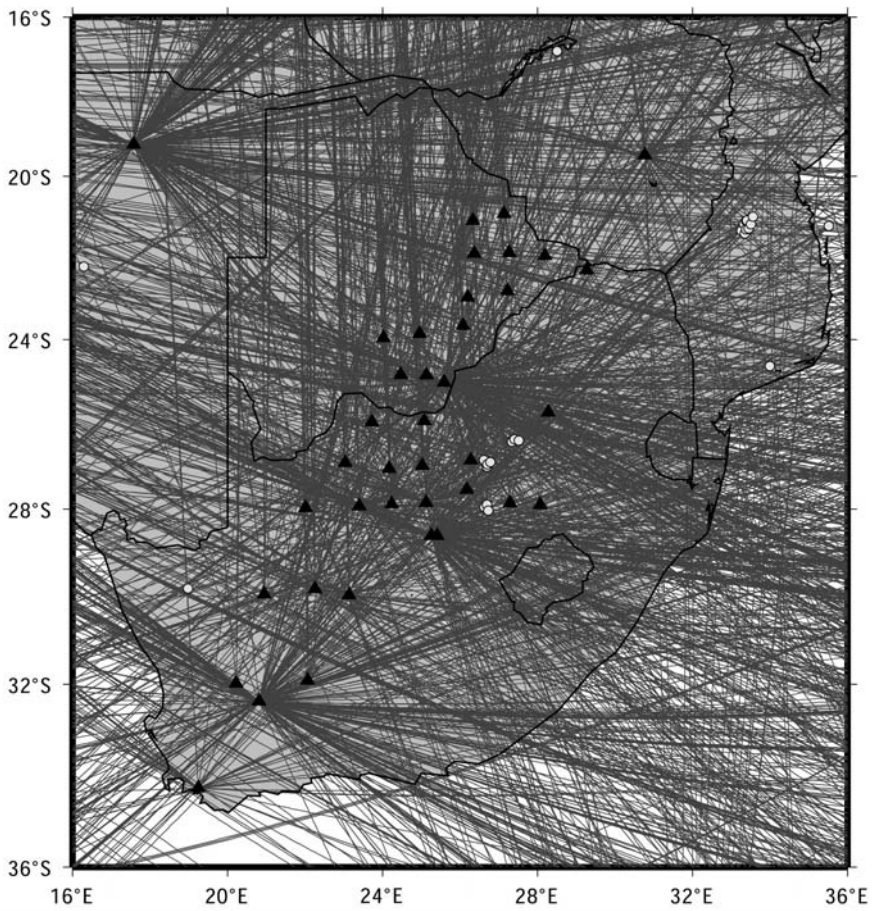

Figure 4. Map showing raypath coverage for 20 s Rayleigh waves used in the revised *Pasyanos and Nyblade* [2007] group velocity model. Station locations are shown with solid triangles, and event locations are shown with white circles. Most of the events are located outside of the area shown in the map.

measurements were made using single station measurements (event to station) and the inversion method used to obtain group velocity maps is based on ray approximation.

[18] For periods of 100 to 175 s, group velocities were taken from the Harvard model [*Larson and Ekström*, 2001]. A single dispersion curve for each station was obtained by first joining the group velocities from 10 to 90 s and 100 to 175 s and then smoothing the composite curve using a 3-point running average. The group velocity measurements from the Harvard model were included in the composite curve so that the 1-D models obtained from the inversions would show mantle structure that is regionally representative of southern Africa.

5. Data Processing and Modeling Methodology

5.1. Receiver Functions

[19] Receiver functions were computed using the iterative deconvolution method of *Ligorría and Ammon* [1999]. The deconvolution procedure equalizes the teleseismic waveforms so that near-source and instrumental effects are removed from the resulting time series [*Langston*, 1979]. Only the radial receiver functions were used in the joint inversion with the Rayleigh wave group velocity curves. The transverse receiver functions are identically zero for isotropic and laterally homogeneous media, and were computed to verify that this is the case for crust and upper mantle structure under each station.

[20] For each station, receiver functions were binned in ray parameter groups from 0.04 to 0.049 s/km, 0.05 to 0.059 s/km and 0.06 to 0.069 s/km. The purpose of grouping the receiver functions according to ray parameter is to properly account for the phase move out due to varying incidence angles [*Cassidy*, 1992; *Gurrola and Minster*, 1998]. Receiver function averages were then computed for each ray parameter bin.

[21] For each teleseismic event, receiver functions were computed at two overlapping frequency bands: a low frequency band of $f \leq 0.5$ Hz (Gaussian bandwidth of 1.0 s), and a high frequency band of $f \leq 1.25$ Hz (Gaussian bandwidth of 2.5 s). The low frequency bandwidth provides a better constraint on longer wavelength features in the subsurface, while the high frequency bandwidth provides a better constraint on shorter wavelength features. The combination of low and high frequency receiver functions help in discriminating sharp versus gradational transitions in the subsurface [*Owens and Zandt*, 1985; *Julià*, 2007].

5.2. Joint Inversion of Receiver Functions and Rayleigh Wave Group Velocities

[22] The joint inversion of receiver functions and surface wave dispersion curves results in 1-D shear wave depth-

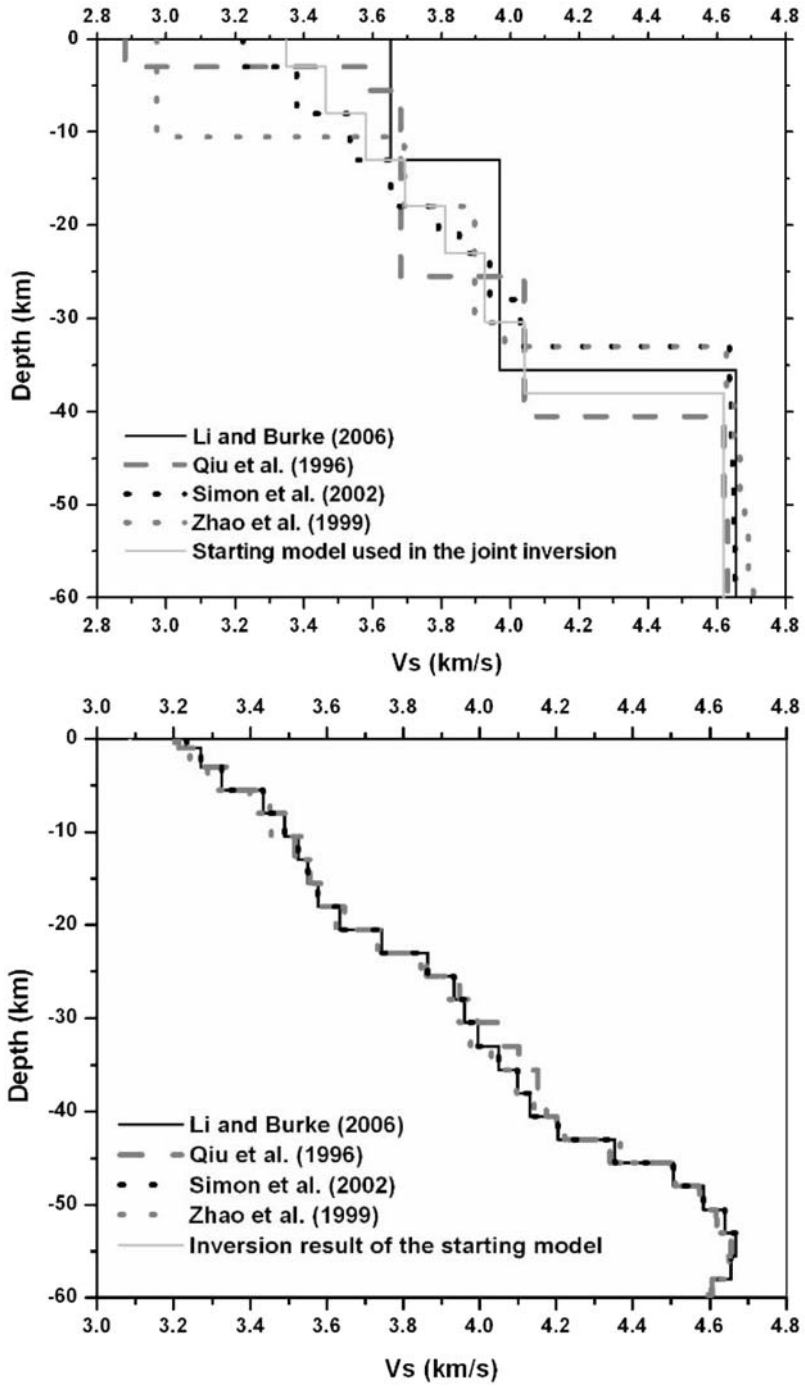

Figure 5. (top) Five different starting models used in the joint inversion algorithm to produce (bottom) velocity models for station SA40. This illustrates that the inversion results are not sensitive to the starting model.

velocity profiles for each recording station [*Julià et al.*, 2000, 2003]. The technique has been widely used to investigate crustal and upper mantle structure in other continental regions, for example, the Arabian shield [*Julià et al.*, 2003], the Tanzania Craton [*Julià et al.*, 2005] and the Ethiopian Plateau [*Dugda et al.*, 2007]. The advantage of jointly inverting receiver functions and surface wave dispersion measurements is that better resolution of the subsurface shear wave velocity structure can be obtained compared to independent inversions of either data set [*Julià et al.*, 2000, 2003].

[23] The joint inversion method makes use of a linearized inversion procedure that minimizes a weighted combination of the L2 norm of the vector residuals corresponding to each data set. The weights consist of a normalization constant that accounts for the different number of data points and different physical units in each data set, as well as an influence parameter that controls the relative influence

of each data set on the inverted model [*Julià et al.*, 2000]. In order to obtain smoothly varying depth-velocity profiles, the objective function also includes a model vector difference norm of the second order differences between adjacent layers [*Ammon et al.*, 1990; *Julià et al.*, 2000].

[24] Influence factors and smoothing parameters were selected for each tectonic domain in order to obtain smooth depth-velocity profiles that match the observations. For most of the stations, a good fit to the data was obtained for an influence factor of 0.5 and a smoothing parameter from zero to 0.2. The smoothing parameter had to be raised as high as 0.3 for some of the stations within the mobile belts, suggesting a greater degree of small-scale heterogeneity.

[25] The model parameterization consisted of 74 layers extending to a depth of 532 km. Layer thicknesses of 1 and 2 km were used for the first and second layer, 2.5 km for layers between 3 and 60.5 km depth, 5 km for layers between 60.5 and 255.5 km depth, and 17 to 40 km for layers below 255.5 km depth. The increase in layer thicknesses with depth corresponds to a decrease in the resolving power of the dispersion velocities with increasing period. The starting model used for the inversions is the PREM model [*Dziewonski and Anderson*, 1981] modified for continental structure above 60.5 km depth (Figure 5). Poisson's ratio in the starting model was set at 0.25 in the crust and mantle to a depth of 86 km, 0.28 between depths of 86–230 km, 0.29 between depths of 230 and 374 km, 0.30 between depths of 374–430 km and 0.29 between depths of 430–532 km. Densities were obtained from P wave velocities using the empirical relationship of *Berteussen* [1977].

5.3. Starting Model Dependence and Trade-Offs

[26] To test the dependence of the inversion results on the starting model, a range of regional models were used as starting models for the inversion [*Qiu et al.*, 1996; *Zhao et al.*, 1999; *Simon et al.*, 2002; *Li and Burke*, 2006]. P wave velocities were computed using the same Vp/Vs ratio as for the starting model. The outcome of this test, illustrated in Figure 5, shows that the inversion results in the 0–60 km depth range are not sensitive to the starting models.

[27] Because long-period group velocities constrain average velocity structure within relatively large depth ranges in the upper mantle, a trade-off exists between shallow and deep structure [e.g., *Julià et al.*, 2005]. To constrain this trade-off, we forward modeled structure below 200 km depth using a trial-and-error process by finding models that best fit the 140–175 s period group velocities. This was done by fixing velocities below 200 km between a range of −5 and +5% of the PREM velocities and then inverting for the velocity structure above 200 km depth. The best fitting model for each station was selected when the predicted group velocities in the 140–175 s range matched the observed group velocities. Figure 6 shows an example for one station with velocities of PREM and −2, −3, −5% PREM below 200 km depth. The best fitting model for this station is −3% PREM. For most of the stations, it was found that a −2% PREM model tends to fit the 140–175 s period group velocities best. However, a −3% PREM model was used for the stations in the Kheis Province, Limpopo Belt, Okwa terrain and Zimbabwe Craton and a −5% PREM model was used for both the NNB and CFB.

5.4. Model Uncertainties

[28] To determine the uncertainties in the model results at crustal depths, we have examined the uncertainty introduced by our selection of model parameters for the inversions as well as by the group velocities taken from the revised *Pasyanos and Nyblade* [2007] model. Following the approach by *Julià et al.* [2005], we estimated the uncertainties in the inversion results from parameter selection by repeating inversions for each station using a range of weighting parameters, constraints and Poisson's ratio. The uncertainties in the shear wave velocities for the crust obtained from this procedure are around 0.1 km/s.

[29] Resolution tests of the revised *Pasyanos and Nyblade* [2007] group velocity model indicate that the spatial resolution at periods most sensitive to crustal structure (∼10–50 s) is 3 to 4 degrees, and thus the revised *Pasyanos and Nyblade* [2007] group velocity model has sufficient resolution to image differences in group velocities between regions that are ∼300 to 400 km wide. To assess the uncertainty in crustal velocities possibly introduced by the group velocity measurements for regions smaller than that, we have taken two dispersion curves from the revised *Pasyanos and Nyblade* [2007] model showing "end-member" high and low group velocities, and have rerun the inversions for many stations using them.

[30] The results are illustrated in Figure 7 for two stations. For station BOSA in the middle of the Kaapvaal Craton, group velocities in the 10–50 s range are lower than for station SA81 in the NNB, and the 1-D inversions for these stations show very different lower crustal structure (Figures 7a and 7c). When the 1D inversion is performed for BOSA using the higher group velocities for SA81, the shear wave velocities increase by 0.1 to 0.2 km/s (Figure 7b). When the 1D inversion is performed for SA81 using the lower group velocities for BOSA, the shear wave velocities decrease by 0.1 to 0.2 km/s. In all four models, the dispersion curves and receiver functions are fit equally well (Figure 7). This exercise indicates that even for regions less than 300 to 400 km wide, at most an uncertainty of 0.1 to 0.2 km/s in shear wave velocity is introduced by using the group velocities from the revised *Pasyanos and Nyblade* [2007] model.

Figure 6. Diagram for station SA55 to illustrate the procedure used for determining structure below 200 km. Shown are different models tested for structure below 200 km depth using velocities from PREM and 2%, 3%, and 5% less than PREM. (a) Observed (black line) and predicted (gray line) group velocity curves. The insets show the fit to the longest period (140–175 s) group velocities for the four different models tested. (b) Observed (black line) and predicted (gray line) receiver functions. (c) The shear wave velocity models obtained from the joint inversion (black line) and the PREM shear wave velocity model (gray line) for reference. The 3% less than PREM model for shear wave velocities below 200 km depth gives the best fit to the longest period group velocities.

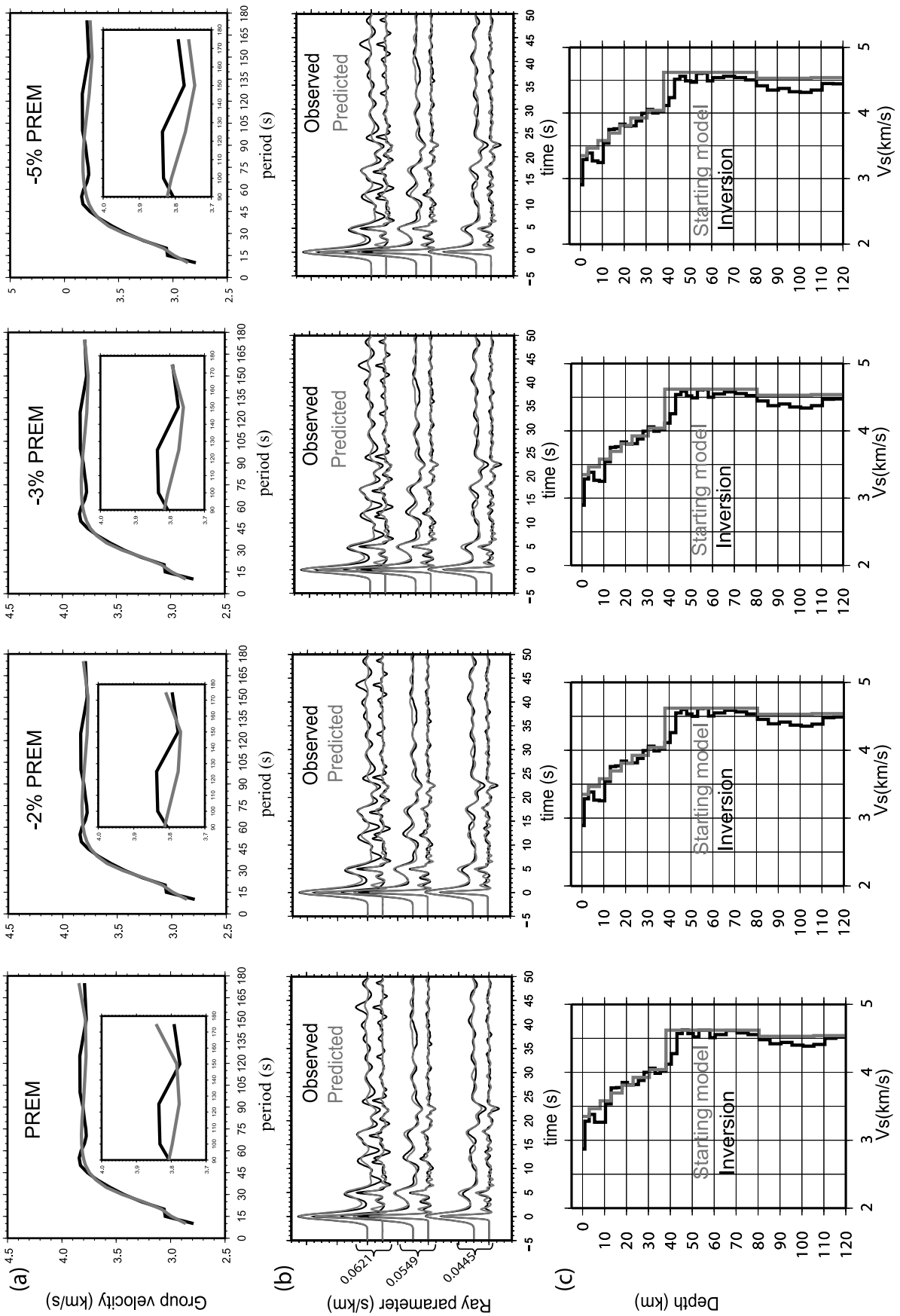
(a)
PREM
-2% PREM
-3% PREM
-5% PREM
Group velocity (km/s)
period (s)
(b)
Observed
Predicted
0.0621
0.0549
0.0445
Ray parameter (s/km)
time (s)
(c)
Starting model
Inversion
Depth (km)
Vs(km/s)

Figure 6

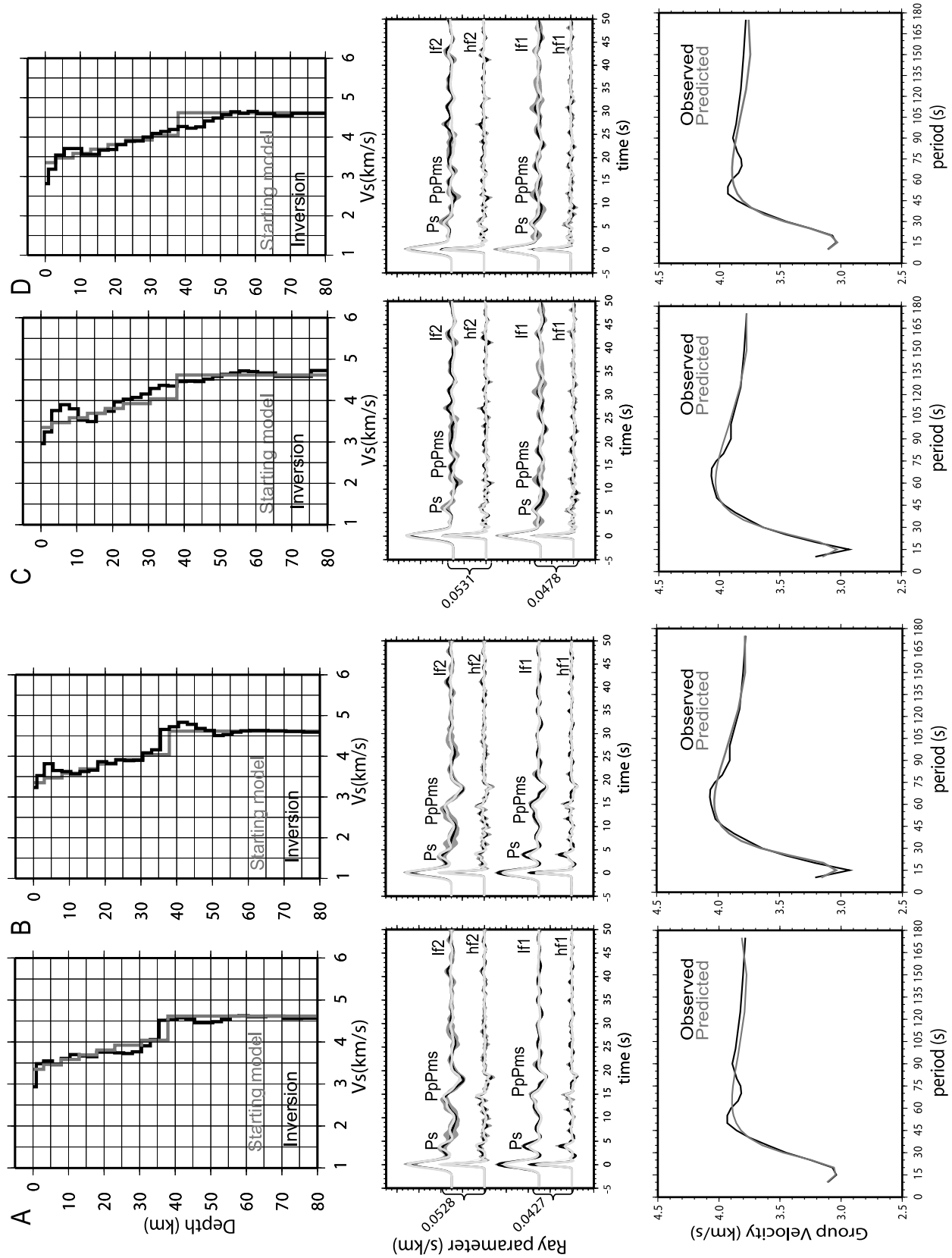
A
B
C
D
Depth (km)
Vs(km/s)
Starting model
Inversion
Ps
PpPms
lf2
hf2
lf1
hf1
0.0528
0.0427
0.0531
0.0478
time (s)
Ray parameter (s/km)
Observed
Predicted
period (s)
Group Velocity (km/s)

Figure 7

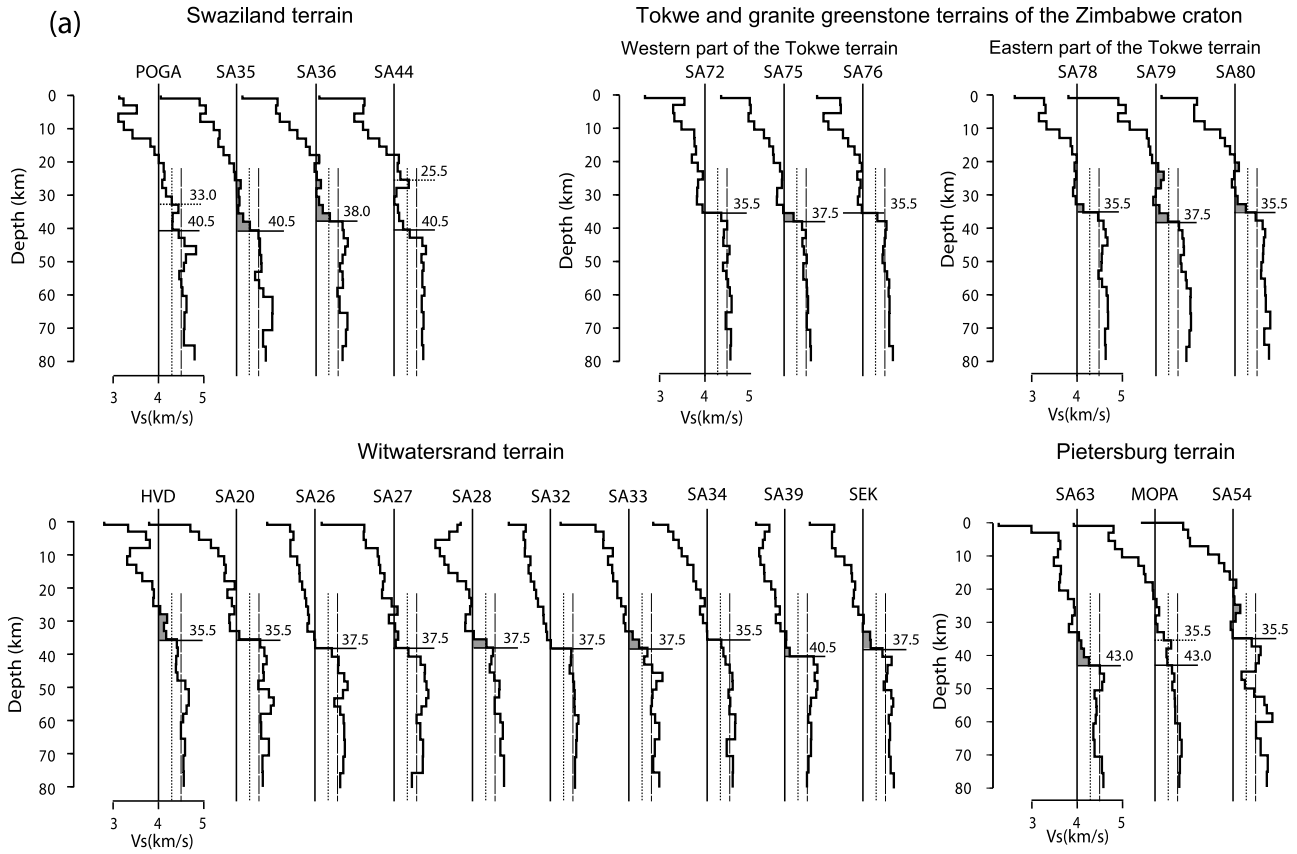

Figure 8. (a–d) Shear wave velocity profiles grouped by tectonic terrain. Moho depths are indicated with horizontal lines and numbers in km. Lower crustal layers with Vs $\geq$ 4.0 km/s are shaded, and reference lines at 4.0 km/s (solid), 4.3 km/s (dotted), and 4.5 km/s (dashed) are shown in each profile. See text for explanation of profiles where two horizontal lines (one dotted and one solid) are shown.

[31] Given these considerations, we place the overall uncertainty in the shear wave velocities at no more than 0.2 km/s for any given crustal layer in the model. This uncertainty in the shear wave velocity translates into an uncertainty of no more than 2 to 3 km in Moho depth for most stations where a velocity discontinuity can be seen between the crust and mantle, and no more than 5 km where a smoothly varying shear wave velocity profile is found, indicating a gradational Moho.

6. Results

[32] For twelve of the 101 stations, the inversions did not yield good fits to the receiver functions, and therefore, results for these stations are not presented or interpreted. The receiver functions are too noisy to obtain good waveform fits at stations SA01, SA02, SA03, SA58, SA69, SA82, SA139, SA155, CNG, while it is difficult to see a Moho Ps conversion on the receiver functions for stations SA07, SA08, SA12 (all in the NNB). The results for the remaining 89 stations are summarized in Figures 8, 9, 10, and 11.

[33] Figures 8a–8d show the shear wave velocity profiles grouped by tectonic terrain, and Table 2 provides a summary of key crustal parameters derived from these profiles. Crustal thickness beneath each station was determined by placing the Moho at the depth where the shear wave velocity exceeds 4.3 km/s. Shear wave velocity ranges for typical lower crustal lithologies obtained by using experimentally determined P wave velocities and Vp/Vs ratios [e.g., *Christensen and Mooney*, 1995; *Christensen*, 1996] show that shear wave velocities in the lower crust cannot

Figure 7. Analysis of uncertainties in the joint inversion results using two stations, BOSA and SA81, with different group velocity curves. (a) Results for BOSA using the group velocities for the location of BOSA from the revised *Pasyanos and Nyblade* [2007] model. (b) Same as Figure 7a but with the group velocities for the location of SA81 in the revised *Pasyanos and Nyblade* [2007] model. (c) Model results for SA81 using the group velocities for the location of SA81 from the revised *Pasyanos and Nyblade* [2007] model. (d) Same as Figure 7c but with the group velocities for the location of BOSA. The top plots show 1-D velocity models from the joint inversion using the receiver functions shown in the middle plots and the group velocities shown in the bottom plots. For the receiver functions, 1σ error bounds are shown with gray shading around the average observed receiver functions (black line) and the predicted receiver functions (light gray line). The high (hf1, hf2) and low (lf1, lf2) frequency receiver functions are grouped in different ray parameter bins.

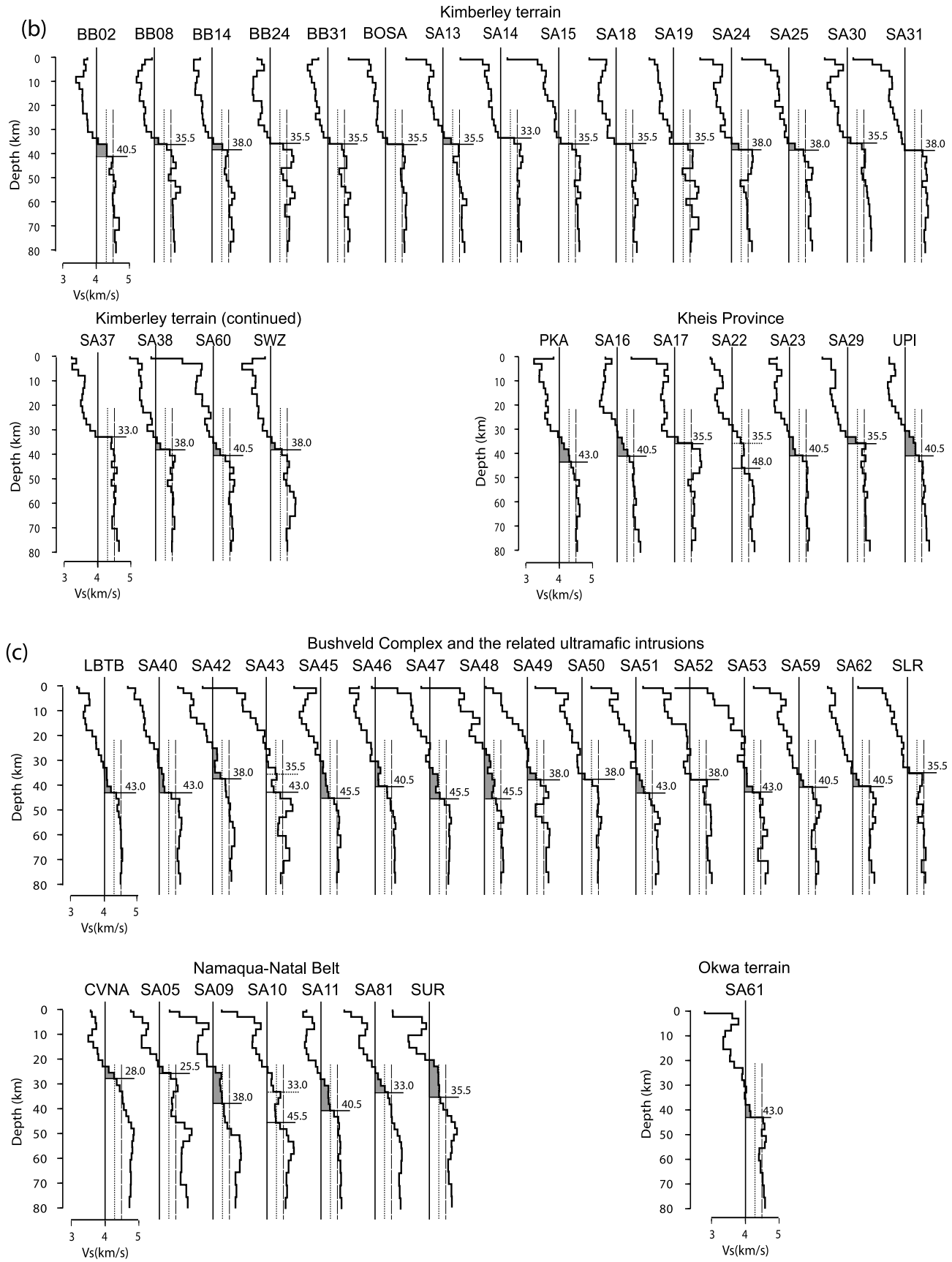

Figure 8. (continued)

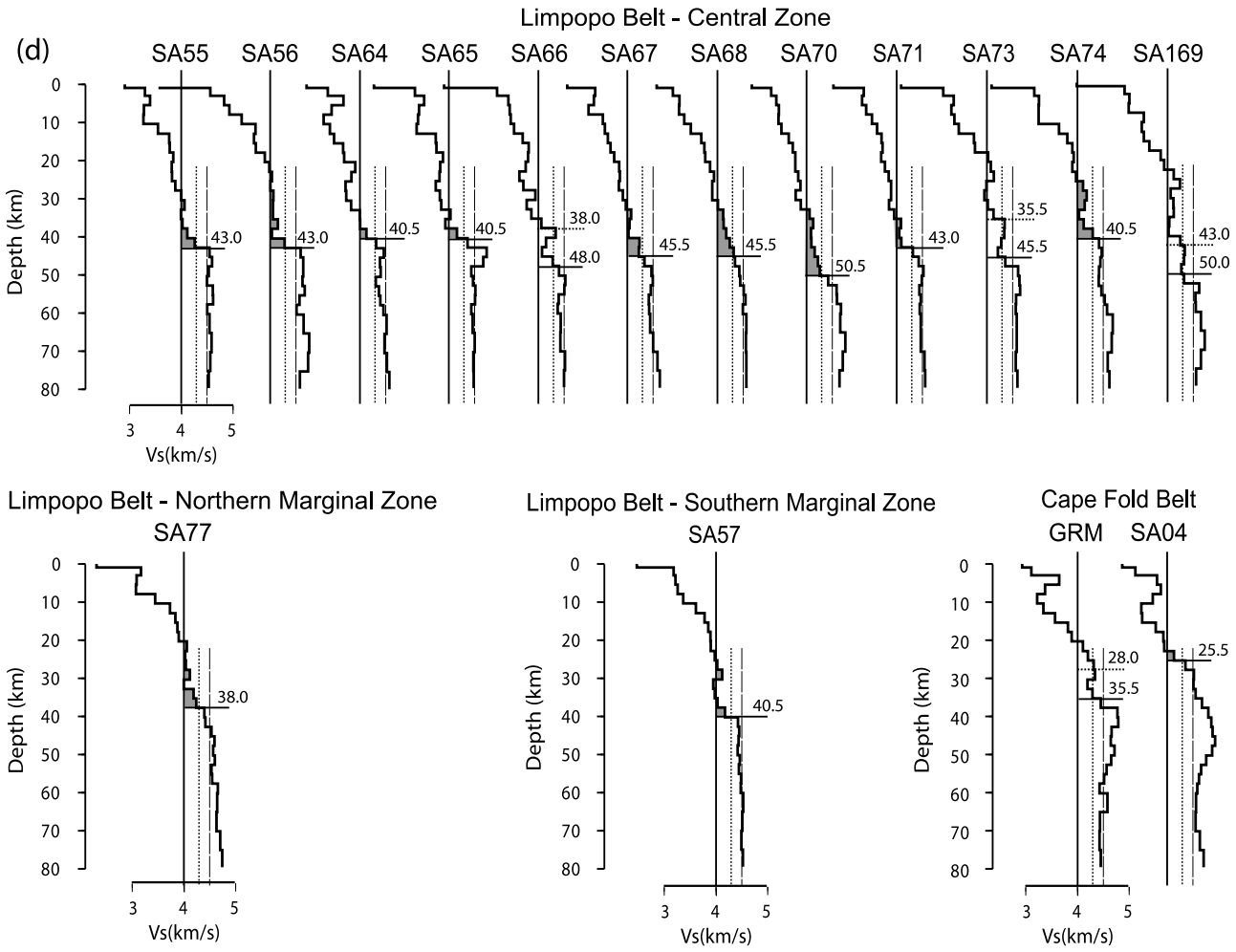

Figure 8. (continued)

be higher than 4.3 km/s. Therefore, we take shear wave velocities above 4.3 km/s to indicate the presence of lithologies with mantle compositions, and we place the Moho where the shear wave velocities exceed that value. For many stations, there is a significant increase in velocity at the depth at which the shear wave velocity exceeds 4.3 km/s, but for other stations the change in shear wave velocity is gradational. In addition, for 10 stations (SA10, SA22, SA43, SA44, SA66, SA73, SA169, GRM, MOPA, POGA) the velocity profiles show two depths where there is an increase in shear wave velocity above 4.3 km/s with a region of velocity less than 4.3 km/s in between. This high-low-high velocity structure is indicated in Figure 8 for the 10 stations by showing the first increase in velocity above 4.3 km/s with a dotted line and the second increase with a solid line. For these 10 stations, we do not attempt to define the Moho and therefore do not use them for further analysis.

[34] Within the reported uncertainties, we find a 1-to-1 correlation between our Moho estimates and those reported by *Nguuri et al.* [2001], *Nguuri* [2004] and *Nair et al.* [2006], except for a handful of stations, which are shown in Figure 9 with solid symbols. Five stations (SA05, SA09, SA49, SA81, SUR) lie more than 5 km above the 1-to-1 correlation line in Figure 9, where our estimates

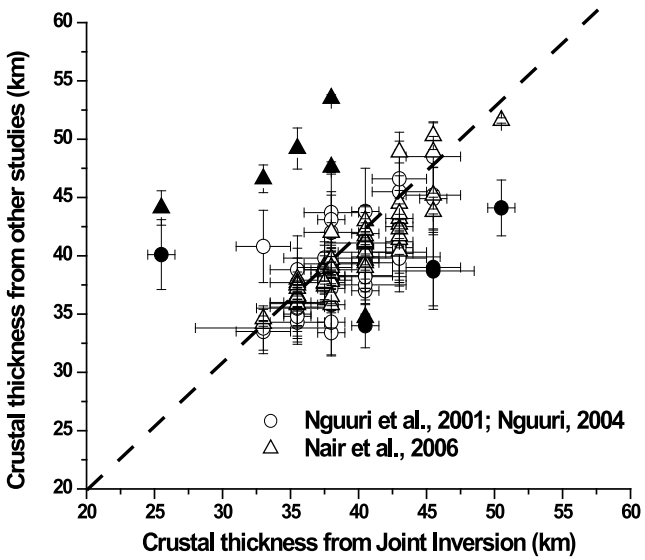

Figure 9. Comparison of crustal thickness estimates from this study with crustal thickness estimates from previous studies. The dashed line shows the 1-to-1 correlation, and the solid symbols show stations that do not fall close ($\geq$5 km) to the 1-to-1 line.

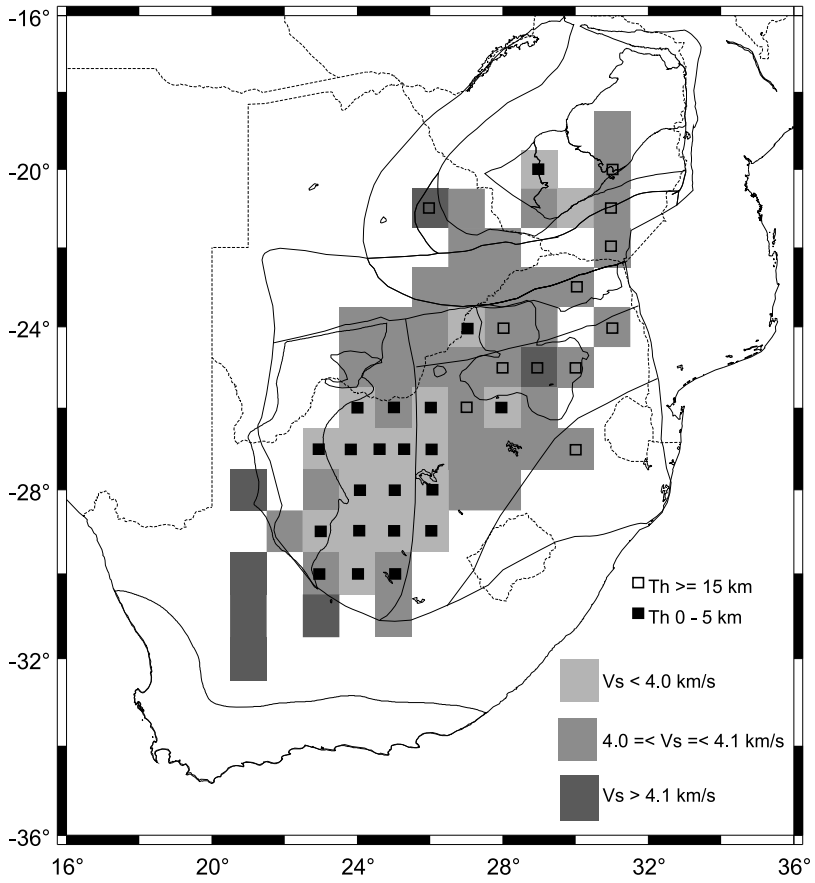

Figure 10. Map showing the average shear wave velocity below 30 km (gray shading) and the average total layer thickness with Vs $\geq$ 4.0 km/s (shown as open and solid squares and denoted as "Th") for 1 x 1 degree blocks. The blocks without symbols are areas where the average total layer thickness with Vs $\geq$ 4.0 km/s is between 5 and 15 km. Solid lines show the outlines of the tectonic terrains from Figure 1.

of Moho depth for these stations are less than those reported by *Nguuri et al.* [2001], *Nguuri* [2004] and *Nair et al.* [2006]. Four stations (SA16, SA47, SA48, SA70) lie more than 5 km below the 1-to-1 correlation line, where our estimates of Moho depth are greater than those reported by *Nguuri et al.* [2001], *Nguuri* [2004] and *Nair et al.* [2006]. The velocity profiles for these stations show complicated lowermost crustal structure commonly with a gradational Moho. We attribute the different Moho depth estimates for these stations to difficulty in identifying the crust-mantle boundary when the velocity structure across this boundary is gradational.

6.1. Lower Crustal Structure

[35] For most terrains, shear wave velocities reach 4.0 km/s or higher over a substantial part of the lower crust (Table 2). The Kimberley terrain and the western part of the Tokwe terrain, however, are different. In these terrains, mean velocities of $\leq$3.9 km/s occur in the lower part of the crust (Table 2). These terrains also have, on average, less than 5 km of high velocity (Vs $\geq$ 4.0 km/s) rock within the lower part of the crust.

[36] The variability in lower crustal structure is illustrated in Figures 10 and 11. In Figure 10, the spatial variability in lower crustal velocity structure is shown for 1 x 1 degree blocks. The mean shear wave velocity below 30 km depth is indicated with shaded boxes, and superimposed on the boxes are symbols showing the thickness of lower crustal layers with Vs $\geq$ 4.0 km/s. The anomalous nature of lower crustal structure in the Kimberley terrain and the western part of the Tokwe terrain is readily apparent. It can also be seen that the anomalous region of lower crustal structure extends beyond the Kimberley terrain into the western part of the Witwatersrand terrain and the eastern part of the Kheis Province. The lack of high velocity rock in the lower parts of the crust in these terrains can also be seen in Figure 8.

6.2. Upper Crustal Structure

[37] A high velocity zone in the upper crust at depths <15 km can be seen in the velocity models for a number of stations (Figure 8). The high velocity zones are isolated features seen on one or two stations in some terrains (e.g., station SA61 in the Okwa terrain), and given the resolution of the revised *Pasyanos and Nyblade* [2007] group velocity model, these isolated upper crustal high velocity zones might not be well imaged. However, for the NNB, a high velocity zone in the upper crust is found over an area wide enough to be resolved by the revised *Pasyanos and Nyblade* [2007] model (Figure 8c). Shear wave velocities within these zones are between 3.7 and 4.0 km/s, and decrease to

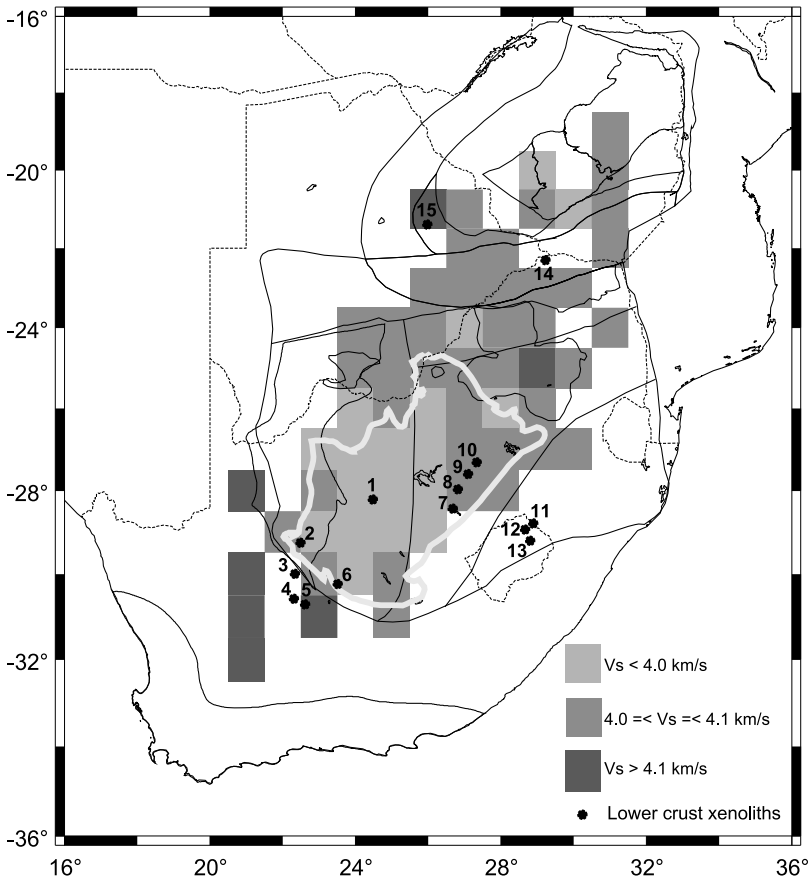

Figure 11. Map showing the average shear wave velocity below 30 km (gray shading), with distribution of the Ventersdorp supergroup (white line) taken from *van der Westhuizen et al.* [2006] and the location of lower crust xenoliths obtained from *Pretorius and Barton* [2003] and *Schmitz and Bowring* [2003a]. The number labels 1–15 represent the names of the kimberlites: 1, Newlands; 2, Markt; 3, Uintjiesberg; 4, Klipfontein-08; 5, Beyersfontein; 6, Lovedale; 7, Star Mine; 8, Kaalvallei; 9, Lace; 10, Voorspoed; 11, Mothae; 12, Letseng-la-Terae; 13, Matsoku; 14, Venetia Mine; and 15, Jwaneng. Terrain boundaries are the same as in Figure 1.

3.5–3.7 km/s below these zones, creating the appearance of a low velocity layer in the midcrust. However, it is the upper crustal velocities that are anomalous, not the midcrustal velocities.

6.3. Mantle Structure

[38] For most of the terrains within both the cratonic areas and mobile belts, the mean shear wave velocity from the Moho to depths of ~60 km is between 4.5 and 4.7 km/s (i.e., uppermost mantle; Table 2). We find little evidence for systematic differences in the uppermost mantle (i.e., the top 10–20 km of the mantle) velocities across southern Africa. As a result of using group velocities for periods >90 s from the Harvard model in the inversions to obtain a regionally representative upper mantle model, mantle structure below ~60–70 km is not sufficiently resolved to comment on variations in lithospheric thickness or sublithospheric mantle structure between terrains.

7. Discussion

[39] Because southern Africa has not experienced a major tectonothermal event since the Karoo flood basalt volcanism at c. 180 Ma, the variability found within the shear wave velocities at lower crustal depths most likely results from compositional differences rather than thermal ones. It is well established from laboratory studies that mafic lithologies commonly found in the continental crust, such as amphibolite, garnet-bearing and garnet-free mafic granulite, and mafic gneiss, have higher shear wave velocities (>3.9 km/s), while intermediate-to-felsic lithologies have lower shear wave velocities (<3.9 km/s) [e.g., *Holbrook et al.*, 1992; *Christensen and Mooney*, 1995; *Rudnick and Fountain*, 1995; *Rudnick and Gao*, 2003].

7.1. Interpretation of Higher Shear Wave Velocities in the Lower Crust

[40] We interpret the crustal layers in our models with shear wave velocities of 4.0 km/s or higher as consisting of predominantly mafic lithologies. *Rudnick and Fountain* [1995] and *Rudnick and Gao* [2003] argued that high velocity (Vp ~ 7.0 km/s, Vs ~ 4.0 km/s), mafic rock is characteristic of the lower crust in many Precambrian terrains globally. Thus, our interpretation is not unprecedented.

[41] *Rudnick and Gao* [2003] also suggest several explanations for the origin of mafic lower crust in Precambrian

Table 2. Summary of Crustal Structure by Geological Terrains Shown in Figures 8 and 10

Terrain	Average Moho Depth ± Standard Deviation (km)	Number of Stations Used	Uppermost Mantle Vs (km/s)	Average Crustal Vs	Average Vs Below 20 km Depth (km/s)	Average Vs Below 30 km Depth (km/s)	Average Thickness of Layers With Vs $\geq$ 4.0 km/s (km)
Kaapvaal Craton							
Witwatersrand	37.2 ± 1.5	10	4.6	3.7	3.9	4.0	7
Swaziland	39.3 ± 1.8	2	4.6	3.7	4.0	4.1	14
Pietersburg	39.3 ± 5.3	2	4.5	3.6	4.0	4.0	12
Kimberley	36.6 ± 2.1	19	4.6	3.7	3.8	3.9	2
Zimbabwe Craton							
Western part of the Tokwe terrain	36.2 ± 1.2	3	4.5	3.6	3.9	3.9	4
Eastern part of the Tokwe terrain	36.2 ± 1.2	3	4.6	3.6	4.0	4.0	12
Bushveld Complex and the related ultramafic intrusions	41.2 ± 3.2	15	4.5	3.7	4.0	4.0	10
Namaqua-Natal Belt	33.4 ± 5.8	6	4.6	3.8	4.1	4.3	12
Limpopo Belt							
SMZ	40.5	1	4.5	3.7	4.0	4.1	15
CZ	43.6 ± 3.3	9	4.5	3.7	4.0	4.1	11
NMZ	38.0	1	4.6	3.7	4.1	4.1	15
Kheis Province	39.3 ± 3.1	6	4.6	3.7	3.9	4.1	7
Okwa terrain	43.0	1	4.5	3.7	3.9	4.0	13
Cape Fold Belt	25.5	1	4.7	3.7	4.0	-	-

terrains, such as basaltic underplating, magmatic intrusion, and tectonomagmatic processes responsible for the formation of Archaean crust. The mafic layer in the lower crust of the BC is likely caused by a combination of magmatic intrusion and underplating. It has been estimated that the total magma volume that has been added to the Bushveld crust is around 0.6×10^6 km^3 [*Von Gruenewaldt et al.*, 1985], thickening the crust by ~5–10 km. The large (>10 km) thickness of mafic rock in the lower parts of the crust in the NNB, the CZ of the Limpopo Belt, parts of the Kheis Province and the CFB can be attributed to suture processes during the formation of these terrains. In Precambrian sutures elsewhere (e.g., the Superior Province [*Gibb et al.*, 1983], the Tanzania Craton [*Nyblade and Pollack*, 1992], the Yilgarn Craton [*Mathur*, 1974; *Wellmann*, 1978], the Indian shield [*Subrahmanyam*, 1978], the Mann shield [*Blot et al.*, 1962; *Louis*, 1978; *Black et al.*, 1979]), 5–10 km of crustal thickening is observed along with the presence of mafic units in a crust commonly affected by granulite facies metamorphism and extraction of a felsic partial melt component. Both the thicker crust and the large thickness of lower crust with high shear wave velocities found in the NNB, CZ, and Kheis Province is consistent with typical "suture" thickened crust found in other Precambrian terrains, and need not be viewed as anomalous.

[42] The mafic lower crust we find in the BC is consistent with Vp/Vs ratios of >1.76 as described by *Nguuri* [2004] and *Nair et al.* [2006] (Table 1). Similarly, the reported Vp/Vs ratios of 1.78 and 1.84 for the NNB and Limpopo Belt, respectively, are consistent with our findings (Table 1).

7.2. Interpretation of Lower Shear Wave Velocities in the Lower Crust

[43] Following the experimental studies of rock velocities discussed above, we interpret the lower shear wave velocities (Vs $\leq$ 3.9 km/s) in the lower parts of the crust in several terrains to indicate the presence of predominantly intermediate-to-felsic lithologies. The lack of mafic material in the lower crust and the mean crustal thickness of 37 km for the Kimberley terrain are consistent with the findings by *Niu and James* [2002]. Our results indicate that the region of low shear wave velocities in the lower crust extends across much of the Kimberley terrain and into parts of the adjacent Kheis Province and Witwatersrand terrain (Figure 10). Low shear wave velocities in the lower crust also occur in the western part of the Tokwe terrain.

[44] To explain an intermediate-to-felsic composition for the lower crust in the Kimberley terrain, as well as the flat Moho that *Niu and James* [2002] observed, *James et al.* [2003] suggested that the crust could have been extensively melted during the Ventersdorp tectonomagmatic event at c. 2.7 Ga. However, it is not clear how melting of the lower crust during the Ventersdorp event would have resulted in the removal of the lower mafic crust unless accompanied by crustal thinning. Figure 11 shows the distribution of the Ventersdorp Supergroup superimposed on the shear wave velocity structure of the lower crust. Most of the areas underlain by intermediate-to-felsic lower crust in South Africa coincide with the region where Ventersdorp rocks have been preserved.

[45] Using seismic reflection profiles, *de Wit and Tinker* [2004] describe Ventersdorp age half graben systems

within the upper crust across the central Kimberley and Witwatersrand terrains. The half grabens are characterized by asymmetrical listric faults that trend east to southeast, and *de Wit and Tinker* [2004] argued that the listric faults are associated with thinning of underlying lower crust. Consequently, regions in the Kaapvaal Craton underlain by an intermediate-to-felsic lower crust may reflect areas where mafic lower crust was either thinned or removed during regional crustal thinning associated with the Ventersdorp event. A similar explanation could be invoked for the low shear wave velocities observed in the lower crust in the western part of the Tokwe terrain, which is overlain by 3.1–2.95 Ga transgressive passive margin and rift sequences [*Jelsma and Dirks*, 2002].

7.3. Crustal Xenoliths

[46] Lower crustal xenoliths in southern Africa are most commonly found within kimberlite pipes [e.g., *Dawson*, 1980; *Nixon*, 1987; *Schmitz and Bowring*, 2003a] (see numbers in Figure 11 for locations). Cratonic lower crustal granulite xenoliths have been described from the Kimberley region (location 1), NNB (locations 2, 3, 4, 5, 6), Free State province (locations 7, 8, 9, 10), northern Lesotho (locations 11, 12, 13) [*Schmitz and Bowring*, 2003a]. Off-craton and craton-margin xenoliths come from the CZ of the Limpopo Belt (location 14) [*Pretorius and Barton*, 2003] and the unexposed extension of the Magondi Belt in north central Botswana (location 15) [*Schmitz and Bowring*, 2003a].

[47] Xenoliths from kimberlite pipes [e.g., *Dawson*, 1980; *Nixon*, 1987; *Schmitz and Bowring*, 2003a] can be used as an independent check on the composition of the lithosphere through which the pipe ascended. In this way, suites of lower crustal xenoliths collected from kimberlite pipes in the Kaapvaal Craton and surrounding mobile belts [*Schmitz and Bowring*, 2003a; *Pretorius and Barton*, 2003] (Figure 11) can be used to confirm the presence or absence of mafic rocks in the lower crust.

[48] Lower crustal xenoliths from the Kimberley terrain are dominated by metapelite, and mafic rocks are absent [*Schmitz and Bowring*, 2003a]. In contrast, mafic granulite xenoliths are common at all of the other localities [*Dawson and Smith*, 1987; *Dawson et al.*, 1997; *Schmitz and Bowring*, 2003a, 2003b] (Figure 11), which is consistent with the variability in the shear wave velocity structure of the lower crust described in this study.

8. Summary

[49] To investigate details of lower crustal structure in southern Africa, we have jointly inverted receiver functions and Rayleigh wave group velocities for broadband seismic stations spanning the greater part of the exposed Precambrian shield of southern Africa. From the joint inversion, 1-D shear wave velocity profiles for the crust and uppermost mantle beneath 89 stations have been obtained.

[50] Within the reported uncertainties, we find a 1-to-1 correlation between our Moho depth estimates and those reported by previous studies [*Nguuri et al.*, 2001; *Nguuri*, 2004; *Nair et al.*, 2006]. The primary new observation that we make is that there is considerable variability in the velocity structure of the lower part of the crust across southern Africa. For most terrains, shear wave velocities reach 4.0 km/s or higher over a large part of the lower crust. In contrast, for much of the Kimberley terrain and adjacent parts of the Kheis Province and Witwatersrand terrain, as well as for the western part of the Tokwe terrain, mean shear wave velocities of $\leq$3.9 km/s characterize the lower part of the crust. The lower shear velocities in the lower crust of the Kimberley terrain are consistent with results from previous studies [*Niu and James*, 2002; *James et al.*, 2003].

[51] Our findings indicate that the lower crust across much of the southern African shield in both Archaean and Proterozoic terrains has a predominantly mafic composition, except for the southwest part of the Kaapvaal Craton and western part of the Zimbabwe Craton, where the lower crust is intermediate to felsic in composition. The mafic layer in the lower crust of the BC is likely caused by a combination of magmatic intrusion and underplating. The large thickness of high shear wave velocity lower crust found in the NNB, CZ, and Kheis Province are consistent with typical "suture" thickened crust found in Precambrian terrains globally.

[52] Most of the areas in the Kaapvaal Craton underlain by intermediate-to-felsic lower crust and a shallower Moho coincide with the region where Ventersdorp rocks have been preserved. This correlation supports the suggestion by *de Wit and Tinker* [2004] that extension along crustal-scale listric fault systems that were active during the Ventersdorp tectonomagmatic event at c. 2.7 Ga could have resulted in the attenuation and local removal of mafic lower crust. A similar explanation could be invoked for the low shear wave velocities observed in the lower crust in the western part of the Tokwe terrain, which is overlain by 3.1–2.95 Ga transgressive passive margin and rift sequences [*Jelsma and Dirks*, 2002]. The absence of mafic xenoliths in the Kimberley terrain and the presence of mafic xenoliths in the other terrains is consistent with the variability in the shear velocity structure of the lower crust found in this study.

[53] **Acknowledgments.** We would like to thank Charles Ammon, Mulugeta Dugda, and Yongcheol Park for assistance with computer codes, Magda Roos for help in digitizing terrain boundaries, and all those who assisted with the Southern African Seismic Experiment. Two anonymous reviewers and an Associate Editor provided comments that helped to improve this paper. E.K. would like to acknowledge support from the Council for Geoscience and the AfricaArray program. This research has been supported by the National Science Foundation (grants EAR 0440032 and OISE 0530062), the AfricaArray program and the South African National Research Foundation. This research was also performed under the auspices of the U.S. Department of Energy by Lawrence Livermore National Laboratory under contract DE-AC52-07NA27344. This is LLNL contribution LLNL-JRNL-408744.

References

Ammon, C. J., G. E. Randall, and G. Zandt (1990), On the nonuniqueness of receiver function inversions, *J. Geophys. Res.*, *95*, 15,303–15,318, doi:10.1029/JB095iB10p15303.

Barton, J. M., Jr., R. E. P. Fripp, P. Horrocks, and N. McLean (1979), The geology, age and tectonic setting of the Messina layered intrusion, Limpopo Mobile Belt, southern Africa, *Am. J. Sci.*, *279*, 1108–1134.

Berger, M., J. D. Kramers, and T. F. Nägler (1995), Geochemistry and geochronology of charno-enderbites in the Northern Marginal Zone of the Limpopo Belt, southern Africa and genetic models, *Schweiz. Mineral. Petrogr. Mitt.*, *75*, 17–42.

Berteussen, K. A. (1977), Moho depth determinations based on spectral ratio analysis, *Phys. Earth Planet. Inter.*, *31*, 313–326.

Black, R., R. Caby, A. Moussine-Pouchkine, J. M. Bertad, A. M. Boullier, J. Fabre, and A. Lesquer (1979), Evidence for late Precambrian plate tectonics in West Africa, *Nature*, *278*, 223–227, doi:10.1038/278223a0.

Bloch, S., A. L. Hales, and M. Landisman (1969), Velocities in the crust and upper mantle of southern Africa from multi-mode surface wave dispersion, *Bull. Seismol. Soc. Am.*, *59*, 1599–1629.

Blot, C., Y. Crenn, and R. Rechenmann (1962), Elements apportes par la gravimetrie a la connaissance de la tectonique profonde du Senegal, *C. R. Hebd. Seances Acad. Sci.*, *254*, 1131–1133.

Carlson, R. W., T. L. Grove, M. J. de Wit, and J. J. Gurney (1996), Program to study crust and mantle of the Archean Craton in southern Africa, *Eos Trans. AGU*, *77*(29), 273–277, doi:10.1029/96EO00194.

Cassidy, J. F. (1992), Numerical experiments in broad-band receiver function analysis, *Bull. Seismol. Soc. Am.*, *82*, 1453–1474.

Cawthorn, R. G., H. V. Eales, F. Walraven, R. Uken, and M. K. Watkeys (2006), The Bushveld complex, in *The Geology of South Africa*, edited by M. R. Johnson, C. R. Anhaeusser, and R. J. Thomas, pp. 261–281, Geol. Soc. of S. Afr., Johannesburg, South Africa.

Christensen, N. I. (1996), Poisson's ratio and crustal seismology, *J. Geophys. Res.*, *101*, 3139–3156, doi:10.1029/95JB03446.

Christensen, N. I., and W. D. Mooney (1995), Seismic velocity structure and composition of the continental crust: A global view, *J. Geophys. Res.*, *100*, 9761–9788, doi:10.1029/95JB00259.

Cornell, D. H., R. J. Thomas, H. F. G. Moen, D. L. Reid, J. M. Moore, and R. L. Gibson (2006), The Namaqua-Natal province, in *The Geology of South Africa*, edited by M. R. Johnson, C. R. Anhaeusser, and R. J. Thomas, pp. 325–379, Geol. Soc. of S. Afr., Johannesburg, South Africa.

Dawson, J. B. (1980), *Kimberlites and Their Xenoliths*, Springer, Berlin.

Dawson, J. B., and J. V. Smith (1987), Reduced sapphirine granulite xenoliths from the Lace kimberlite, South Africa: Implications for the deep structure of the Kaapvaal Craton, *Contrib. Mineral. Petrol.*, *95*, 376–383, doi:10.1007/BF00371851.

Dawson, J. B., S. L. Harley, R. L. Rudnick, and T. R. Irel (1997), Equilibration and reaction in Archaean quartz-sapphirine granulite xenoliths from the Lace kimberlite pipe, South Africa, *J. Metamorph. Geol.*, *15*, 253–266, doi:10.1111/j.1525-1314.1997.00017.x.

de Wit, M. J., and J. Tinker (2004), Crustal structures across the central Kaapvaal Craton from deep-seismic reflection data, *S. Afr. J. Geol.*, *107*, 185–206, doi:10.2113/107.1-2.185.

de Wit, M. J., C. Roering, R. J. Hart, R. A. Armstrong, C. E. J. Ronde, R. W. E. Green, M. Tredoux, E. Peberdy, and R. A. Hart (1992), Formation of an Archaean continent, *Nature*, *357*, 553–562, doi:10.1038/357553a0.

Dirks, P. H. G. M., and H. A. Jelsma (2002), Crust-mantle decoupling and the growth of the Archaean Zimbabwe Craton, *J. Afr. Earth Sci.*, *34*, 157–166, doi:10.1016/S0899-5362(02)00015-5.

Dugda, M. T., A. A. Nyblade, and J. Julia (2007), Thin lithosphere beneath the Ethiopian Plateau revealed by a joint inversion of Rayleigh wave group velocities and receiver functions, *J. Geophys. Res.*, *112*, B08305, doi:10.1029/2006JB004918.

Durrheim, R. J., and R. W. E. Green (1992), A seismic refraction investigation of the Archaean Kaapvaal Craton, South Africa, using the mine tremors as the energy source, *Geophys. J. Int.*, *108*, 812–832, doi:10.1111/j.1365-246X.1992.tb03472.x.

Dziewonski, A. M., and D. L. Anderson (1981), Preliminary reference Earth model, *Phys. Earth Planet. Inter.*, *25*, 297–356, doi:10.1016/0031-9201(81)90046-7.

Eglington, B. M., and R. A. Armstrong (2004), The Kaapvaal Craton and adjacent orogens, southern Africa: A geochronological database and overview of the geological development of the craton, *S. Afr. J. Geol.*, *107*, 13–32, doi:10.2113/107.1-2.13.

Gane, P. G., H. J. Logie, and J. H. Stephen (1949), Triggered telerecording seismic equipment, *Bull. Seismol. Soc. Am.*, *39*, 117–143.

Gane, P. G., A. R. Atkins, J. P. F. Sellschop, and P. Seligman (1956), Crustal structure in the Transvaal, *Bull. Seismol. Soc. Am.*, *46*, 293–316.

Gibb, R. A., M. D. Thomas, P. Lapointe, and M. Mukhopadhay (1983), Geophysics of proposed Proterozoic sutures in Canada, *Precambrian Res.*, *19*, 349–384, doi:10.1016/0301-9268(83)90021-9.

Green, R. W. E., and R. J. Durrheim (1990), A seismic refraction investigation of the Namaqualand metamorphic complex, South Africa, *J. Geophys. Res.*, *95*(B12), 19,927–19,932, doi:10.1029/JB095iB12p19927.

Gurrola, H., and J. B. Minster (1998), Thickness estimates of the upper-mantle transition zone from bootstrapped velocity spectrum stacks of receiver functions, *Geophys. J. Int.*, *133*, 31–43, doi:10.1046/j.1365-246X.1998.1331470.x.

Hales, A. L., and I. S. Sacks (1959), Evidence for an intermediate layer from crustal structure studies in the eastern Transvaal, *Geophys. J. R. Astron. Soc.*, *2*, 15–33.

Harvey, J. D., M. J. de Wit, J. Stankiewicz, and C. M. Doucouré (2001), Structural variations of the crust in the Southwestern Cape, deduced from seismic receiver functions, *S. Afr. J. Geol.*, *104*, 231–242, doi:10.2113/1040231.

Hatton, C. J., and J. K. Schweitzer (1995), Evidence for synchronous extrusive and intrusive Bushveld magmatism, *J. Afr. Earth Sci.*, *21*, 579–594, doi:10.1016/0899-5362(95)00103-4.

Holbrook, W. S., W. D. Mooney, and N. I. Christensen (1992), The seismic velocity structure of the deep continental crust, in *Continental Lower Crust*, edited by D. M. Fountain, R. Arculus, and R. W. Kay, chap. 1, pp. 1–43, Elsevier, Amsterdam.

James, D. E., F. Niu, and J. Rokosky (2003), Crustal structure of the Kaapvaal Craton and its significance for early crustal evolution, *Lithos*, *71*, 413–429, doi:10.1016/j.lithos.2003.07.009.

Jelsma, H. A., and P. H. G. M. Dirks (2002), Neoarchaean tectonic evolution of the Zimbabwe Craton, in *The Early Earth: Physical, Chemical, and Biological Development*, edited by C. M. R. Fowler, C. J. Ebinger, and C. J. Hawkesworth, *Geol. Soc. Spec. Publ.*, *199*, 183–211.

Johnson, M. R., C. R. Anhaeusser, and R. J. Thomas (Eds.) (2006), *The Geology of South Africa*, 691 pp., Geol. Soc. of S. Afr., Johannesburg, South Africa.

Julià, J. (2007), Constraining velocity and density contrasts across the crust-mantle boundary with receiver function amplitudes, *Geophys. J. Int.*, *171*, 286–301, doi:10.1111/j.1365-2966.2007.03502.x.

Julià, J., C. J. Ammon, R. B. Hermann, and A. M. Correig (2000), Joint inversion of receiver functions and surface-wave dispersion observations, *Geophys. J. Int.*, *143*, 99–112, doi:10.1046/j.1365-246x.2000.00217.x.

Julià, J., C. J. Ammon, and R. B. Hermann (2003), Lithospheric structure of the Arabian Shield from the joint inversion of receiver functions and surface-wave group velocities, *Tectonophysics*, *371*, 1–21, doi:10.1016/S0040-1951(03)00196-3.

Julià, J., C. J. Ammon, and A. A. Nyblade (2005), Evidence for mafic lower crust in Tanzania, East Africa from joint inversion of receiver functions and Rayleigh wave dispersion velocities, *Geophys. J. Int.*, *162*, 555–569, doi:10.1111/j.1365-246X.2005.02685.x.

Kramers, J. D., S. McCourt, and D. D. van Reenen (2006), The Limpopo Belt, in *The Geology of South Africa*, edited by M. R. Johnson, C. R. Anhaeusser, and R. J. Thomas, pp. 209–236, Geol. Soc. of S. Afr., Johannesburg, South Africa.

Kreissig, K., T. F. Nägler, J. D. Kramers, D. D. Van Reenen, and C. A. Smit (2000), An isotopic and geochemical study of the northern Kaapvaal Craton and the Southern Marginal Zone of the Limpopo Belt: Are they juxtaposed terrains?, *Lithos*, *50*, 1–25, doi:10.1016/S0024-4937(99)00037-7.

Kwadiba, M. T. O. G., C. Wright, E. M. Kgaswane, R. E. Simon, and T. K. Nguuri (2003), Pn arrivals and lateral variations of Moho geometry beneath the Kaapvaal Craton, *Lithos*, *71*, 393–411, doi:10.1016/j.lithos.2003.07.008.

Langston, C. A. (1979), Structure under Mount Rainier, Washington, inferred from teleseismic body waves, *J. Geophys. Res.*, *84*, 4749–4762, doi:10.1029/JB084iB09p04749.

Larson, E. W. F., and G. Ekström (2001), Global models of surface wave group velocity, *Pure Appl. Geophys.*, *158*(8), 1377–1400, doi:10.1007/PL00001226.

Li, A., and K. Burke (2006), Upper mantle structure of southern Africa from Rayleigh wave tomography, *J. Geophys. Res.*, *111*, B10303, doi:10.1029/2006JB004321.

Ligorría, J. P., and C. J. Ammon (1999), Iterative deconvolution and receiver function estimation, *Bull. Seismol. Soc. Am.*, *89*, 1359–1400.

Louis, P. (1978), Gravimetrie et geologie en Afrique occidentale et centrale, *Mem. BRGM*, *91*, 53–61.

Mathur, S. P. (1974), Crustal structure in southwestern Australia from seismic and gravity data, *Tectonophysics*, *24*, 151–182, doi:10.1016/0040-1951(74)90135-8.

McCourt, S., and R. A. Armstrong (1998), SIMS U-Pb zircon geochronology of granites from the Central Zone, Limpopo Belt, southern Africa: Implications for the age of the Limpopo Orogeny, *S. Afr. J. Geol.*, *101*, 329–338.

McCourt, S., P. Hilliard, R. A. Armstrong, and H. Munyanyiwa (2001), SHRIMP U-Pb zircon geochronology of the Hurungwe granite northwest Zimbabwe: Age constraints on the timing of the Magondi orogeny and implications for the correlation between the Kheis and Magondi belts, *S. Afr. J. Geol.*, *104*, 39–46, doi:10.2113/104.1.39.

Moen, H. F. G. (1999), The Kheis tectonic subprovince, southern Africa: A lithostratigraphic perspective, *S. Afr. J. Geol.*, *102*, 27–42.

Nair, S. K., S. S. Gao, K. H. Liu, and P. G. Silver (2006), Southern African crustal evolution and composition: Constraints from receiver function studies, *J. Geophys. Res.*, *111*, B02304, doi:10.1029/2005JB003802.

Newton, A. R., R. W. Shone, and P. W. K. Booth (2006), The Cape Fold Belt, in *The Geology of South Africa*, edited by M. R. Johnson, C. R. Anhaeusser, and R. J. Thomas, pp. 521–530, Geol. Soc. of S. Afr., Johannesburg, South Africa.

Nguuri, T. (2004), Crustal structure of the Kaapvaal Craton and surrounding mobile belts: Analysis of teleseismic P waveforms and surface wave

inversions, Ph.D. dissertation, Univ. of the Witwatersrand, Johannesburg, South Africa.

Nguuri, T. K., J. Gore, D. E. James, S. J. Webb, C. Wright, T. G. Zengeni, O. Gwavava, J. A. Snoke, and Kaapvaal Seismic Group (2001), Crustal structure beneath southern Africa and its implications for the formation and evolution of the Kaapvaal and Zimbabwe cratons, *Geophys. Res. Lett.*, *28*(13), 2501–2504, doi:10.1029/2000GL012587.

Niu, F., and D. E. James (2002), Fine structure of the lowermost crust beneath the Kaapvaal Craton and its implications for crustal formation and evolution, *Earth Planet. Sci. Lett.*, *200*, 121–130, doi:10.1016/S0012-821X(02)00584-8.

Nixon, P. H. (1987), Kimberlitic xenoliths and their cratonic setting, in *Mantle Xenoliths*, edited by P. H. Nixon, pp. 215–239, John Wiley, Chichester, U. K.

Nyblade, A. A., and H. N. Pollack (1992), A gravity model for the lithosphere in western Kenya and northeastern Tanzania, *Tectonophysics*, *212*, 257–267, doi:10.1016/0040-1951(92)90294-G.

Owens, T. J., and G. Zandt (1985), The response of the continental crust-mantle boundary observed on broadband teleseismic receiver functions, *Geophys. Res. Lett.*, *12*, 705–708.

Pasyanos, M. E., and A. A. Nyblade (2007), A top to bottom lithospheric study of Africa and Arabia, *Tectonophysics*, *444*(1–4), 27–44, doi:10.1016/j.tecto.2007.07.008.

Pretorius, W., and J. M. Barton Jr. (2003), Measured and calculated compressional wave velocities of crustal and upper mantle rocks in the Central Zone of the Limpopo Belt, South Africa—Implications for lithospheric structure, *S. Afr. J. Geol.*, *106*, 205–212, doi:10.2113/106.2-3.205.

Qiu, X., K. Priestley, and D. McKenzie (1996), Average lithospheric structure of southern Africa, *Geophys. J. Int.*, *127*(3), 563–581, doi:10.1111/j.1365-246X.1996.tb04038.x.

Ransome, I. G. D., and M. J. de Wit (1992), Preliminary investigations into a microplate model for the South Western Cape, in *Inversion Tectonics of the Cape Fold Belt, Karoo and Cretaceous Basins of Southern Africa*, edited by M. J. de Wit and I. G. D. Ransome, pp. 257–266, A. A. Balkema, Rotterdam, Netherlands.

Rudnick, R. L., and D. M. Fountain (1995), Nature and composition of the continental crust: A lower crustal perspective, *Rev. Geophys.*, *33*(3), 267–309, doi:10.1029/95RG01302.

Rudnick, R. L., and S. Gao (2003), Composition of the continental crust, in *Treatise on Geochemistry*, vol. 3, *The Crust*, edited by H. D. Holland and K. K. Turekian, pp. 1–64, doi:10.1016/B0-08-043751-6/03016-4Elsevier, Amsterdam.

Schmitz, M. D., and S. A. Bowring (2003a), Constraints on the thermal evolution of continental lithosphere from U-Pb accessory mineral thermochronometry of lower crustal xenoliths, southern Africa, *Contrib. Mineral. Petrol.*, *144*, 592–618.

Schmitz, M. D., and S. A. Bowring (2003b), Ultrahigh-temperature metamorphism in the lower crust during Neoarchean Ventersdorp rifting and magmatism, Kaapvaal Craton, southern Africa, *Geol. Soc. Am. Bull.*, *115*, 533–548, doi:10.1130/0016-7606(2003)115<0533:UMITLC>2.0.CO;2.

Simon, R. E., C. Wright, E. M. Kgaswane, and M. T. O. Kwadiba (2002), The *P* wavespeed structure below and around the Kaapvaal Craton to depths of 800 km, from traveltimes and waveforms of local and regional earthquakes and mining-induced tremors, *Geophys. J. Int.*, *151*, 132–145, doi:10.1046/j.1365-246X.2002.01751.x.

South African Committee for Stratigraphy (1980), *Stratigraphy of South Africa. Part 1: Lithostratigraphy of the Republic of South Africa, South West Africa/Namibia, and the Republics of Bophuthatswana, Transkei, and Venda*, *Handb. Geol. Surv. S. Afr.*, vol. 8, 690 pp., Dep. of Miner. and Energy Affairs, Repub. of S. Afr., Pretoria, South Africa.

Stankiewicz, J., S. Chevrot, R. D. van der Hilst, and M. J. de Wit (2002), Crustal thickness, discontinuity depth, and upper mantle structure beneath southern Africa: Constraints from body wave conversions, *Phys. Earth Planet. Inter.*, *130*, 235–251, doi:10.1016/S0031-9201(02)00012-2.

Stowe, C. W. (1986), Synthesis and interpretation of structures along the north-eastern boundary of the Namaqua tectonic province, South Africa, *Trans. Geol. Soc. S. Afr.*, *89*, 185–198.

Stowe, C. W. (1989), Discussion on "The Proterozoic Magondi Belt in Zimbabwe—A review," *S. Afr. J. Geol.*, *92*, 69–71.

Subrahmanyam, C. (1978), On the relation of gravity anomalies to geotectonics of the Precambrian terrains of the South Indian shield, *J. Geol. Soc. India*, *19*, 251–263.

Thamm, A. G., and M. R. Johnson (2006), The Cape Supergroup, in *The Geology of South Africa*, edited by M. R. Johnson, C. R. Anhaeusser, and R. J. Thomas, pp. 443–460, Geol. Soc. of S. Afr., Johannesburg, South Africa.

van der Westhuizen, W. A., H. de Bruiyn, and P. G. Meintjes (2006), The Ventersdorp Supergroup, in *The Geology of South Africa*, edited by M. R. Johnson, C. R. Anhaeusser, and R. J. Thomas, pp. 187–208, Geol. Soc. of S. Afr., Johannesburg, South Africa.

Von Gruenewaldt, G., M. R. Sharpe, and C. J. Hatton (1985), The Bushveld complex: Introduction and review, *Econ. Geol.*, *80*, 803–812, doi:10.2113/gsecongeo.80.4.803.

Webb, S. J., R. G. Cawthorn, T. K. Nguuri, and D. E. James (2004), Gravity modeling of Bushveld complex connectivity supported by Southern African Seismic Experiment results, *S. Afr. J. Geol.*, *107*, 207–218, doi:10.2113/107.1-2.207.

Wellmann, P. (1978), Gravity evidence for abrupt changes in the mean crustal density at the junction of Australian crustal blocks, *Aust. Bur. Miner. Resour. Geol. Geophys. Bull.*, *3*, 153–162.

Willmore, P. L., A. L. Hales, and P. G. Gane (1952), A seismic investigation of crustal structure in the western Transvaal, *Bull. Seismol. Soc. Am.*, *42*, 53–80.

Wright, C., E. M. Kgaswane, M. T. O. Kwadiba, R. E. Simon, T. K. Nguuri, and R. McRae-Samuel (2003), South African seismicity, April 1997–April 1999, and regional variations in the crust and uppermost mantle of the Kaapvaal Craton, *Lithos*, *71*, 369–392, doi:10.1016/S0024-4937(03)00122-1.

Zhao, M., C. A. Langston, A. A. Nyblade, and T. J. Owens (1999), Upper mantle velocity structure beneath southern Africa from modeling regional seismic data, *J. Geophys. Res.*, *104*(B3), 4783–4794, doi:10.1029/1998JB900058.

P. H. G. M. Dirks, School of Earth and Environmental Sciences, James Cook University, Townsville, Qld 4811, Australia.

R. J. Durrheim, Council for Scientific and Industrial Research, corner of Rustenburg and Carlow Roads, Johannesburg 0001, South Africa.

J. Julià and A. A. Nyblade, Department of Geosciences, Pennsylvania State University, University Park, PA 16802, USA.

E. M. Kgaswane, Council for Geoscience, 280 Pretoria Rd., Private Bag X112, Pretoria 0001, South Africa. (ekgaswane@geoscience.org.za)

M. E. Pasyanos, Lawrence Livermore National Laboratory, 7000 East Ave., Livermore, CA 94550, USA.